



Utilization of bottom ash waste as a granular column to enhance the lateral load capacity of soft kaolin clay soil

Muhammad Syamsul Imran Zaini¹ · Muzamir Hasan¹ · Wan Nursyafiqah Binti Wan Jusoh¹

Received: 17 October 2022 / Accepted: 11 February 2023

© The Author(s), under exclusive licence to Springer-Verlag GmbH Germany, part of Springer Nature 2023

Abstract

Implementation of industrial wastes such as bottom ash in ground improvement can be cost-effective and environment-friendly. Ground improvement is an effective method of mitigation to improve problematic soils including soft kaolin clay soils as the problematic soils always expose to the severe settlements, low shear strength, immoderate plasticity, greater compressibility, dispersivity, bulging, erodibility, and susceptibility to climatic variables. Several studies conducted on the granular column using the bottom ash column. However, only a few studies have reported findings coherent with the statistical analysis. In this study, the lateral load capacity of bottom ash column-kaolin clay has been conducted. Coherently, the reinforced kaolin clay samples were tested via particle size distribution, Atterberg limit test, relative density, compaction test, permeability test, unconfined compression test, and unconsolidated undrained triaxial test with the single and group of encapsulated bottom ash columns with the geotextile encasement and a prediction model was developed. The effect of a number of columns, column diameter, column height, area replacement ratio, height penetration ratio, height-diameter column ratio, volume replacement ratio, and confining pressures on the shear strength of the single and group of encapsulated bottom ash columns have been investigated. The findings showed the effectiveness of using the bottom ash columns at various number of column, column diameter, column height, area replacement ratio, height penetration ratio, height-diameter column ratio, volume replacement ratio, and confining pressures can enhance the shear strength of the soil up to 77.00% at the optimal utilization of single encapsulated bottom ash column of 10-mm diameter and 80-mm height. Therefore, the study proved that the utilization of bottom ash waste as a granular column can significantly enhance the lateral load capacity of soft kaolin clay soil.

Keywords Ground improvement · Soft kaolin clay · Bottom ash · Shear strength · Engineering properties

Introduction

Soft clay soil is one of the complex soils encompassing parts of the ground comprising numerous valley and coastline areas where countless metropolitan and industrialized areas are found and are regularly confronted in construction projects (Hamidi & Marandi, 2018; Hasan et al., 2021a). Some of the key basic engineering properties and strength difficulties

connected with these forms of soils include severe settlements, low shear strength, immoderate plasticity, greater compressibility, dispersivity, bulging, erodibility, and susceptibility to climatic variables (Zaini et al., 2022a; Chemedda et al., 2018). Kaolin minerals, illite, and smectites are the utmost prevalent types of clay minerals (Mohammed et al., 2021a). Kaolin minerals are mutually the most delicately scattered of superior resistive clays (Vakalova et al., 2018; Hasan et al., 2021a). Therefore, unstable soils for instance, soft kaolin clay soils were modified to alter the engineering characteristics and increase the shear strength of the soils (Hamidi et al., 2018; Vakalova et al., 2018). In the studies made by Phanikumar & Ramanjaneya (2020), structural engineering constructions erected on soft clays, consequently, undergo harmful cracking leading to a heavy cost loss. Phanikumar & Ramanjaneya (2020) calculated that the financial loss induced by soft clay soils was several millions of dollars in the USA, many

Responsible Editor: Philippe Garrigues

✉ Muzamir Hasan
muzamir@ump.edu.my

Muhammad Syamsul Imran Zaini
syamsulimran94@gmail.com

¹ Present Address: Faculty of Civil Engineering Technology, Universiti Malaysia Pahang, Lebuhr Persiaran Tun Khalil Yaakob, 26300 Kuantan, Pahang, Malaysia

thousands of pounds in Britain, and hundreds of millions of rupees in India. Hence, the financial loss produced by soft clay soils is equivalent to financial loss imposed by most or numerous of the natural hazards combined (Hasan et al., 2021a; Zaini et al., 2022b). Due to that, several methods have been suggested by the previous researcher, such as soil stabilization (Hasan et al., 2021a; Zaini et al., 2022b), ground improvement (Bozyigit et al., 2021; Hasan et al., 2021b; Mohammed et al., 2021b), and enhancing the engineering characteristics and shear strength of the problematic soils.

In this study, the ground improvement technique, employing concrete (Ali et al., 2022) or granular inclusion (Wang et al., 2022) in either partially saturated or fully saturated which jointly create a reinforced ground, has been extensively utilized to boost the strength, minimize the settlement, and regulate the movement of the ground (Rezaei-Hosseiniabadi et al., 2022a, Rezaei-Hosseiniabadi et al., 2022b). Simultaneously, the complex ground has been utilized broadly to increase ground-bearing capacity and speed the consolidation of soils (Wang et al., 2022). The ground improvements by granular columns have numerous benefits, such as decreased compressibility and destabilization potential, and greater load-bearing capacity and porosity (Rezaei-Hosseiniabadi et al., 2022a, Rezaei-Hosseiniabadi et al., 2022b). The most significant elements impacting the efficiency of granular columns are the width, arrangement, and interval of columns, granulated component properties, proportional compression of column material, and horizontal restraints given by the underlying soil (Verma & Sahu, 2019; Hosseiniabadi et al., 2019). Nevertheless, the usage of granulated columns in soils with a shear endurance of less than 14 kPa may not be particularly successful owing to the inadequate laterally support supplied by the overlying soft soil (Orekanti & Dommaraju, 2019; Rezaei-Hosseiniabadi et al., 2022a, Rezaei-Hosseiniabadi et al., 2022b). Besides, this constraint can be solved by applying an industrial waste materials encasement such as bottom ash, masonry, and encased steel slag column to the granular column, which offers extra restraints, resulting in the deployment of stronger shear endurance and avoiding significantly swollen column (Orekanti & Dommaraju, 2019; Hilal & Hadzima-Nyarko, 2021). Consequently, for a greater conception, it is vital to offer a sound scientific core for the development of unsaturated ground remedies with impermeable column insertion (Mistry et al., 2021).

For both ecological and financial (Hamada et al., 2022) considerations and in a setting of an annular budget, it is vital to employ regional material for the ground improvement technique. Recently, research has been performed addressing the utilization of industrial waste in civil projects as an option for cost-saving construction resources and resource-efficient (Rezaei-Hosseiniabadi et al., 2022a, Rezaei-Hosseiniabadi et al., 2022b; Kererat et al., 2022). Numerous research emphasized on exploitation of industrial waste materials for instance fiber

waste materials, blast furnace slag, fly ash, rubber shreds, etc., as substitute materials for ground enhancement (Russo et al., 2022; Rezaei-Hosseiniabadi et al., 2022a, Rezaei-Hosseiniabadi et al., 2022b). As stated by Tambara Júnior et al., (2022), the IEA World Energy Balances coal report shows a worldwide data rise in the usage of coal resources throughout 2016 and 2018, surpassing 10,000 TWh. In 2019, there was a minor reduction of 3% in coal energy generation. Although in 2020, coal production decreased marginally in nations such as China and India, it still constitutes the highest share of worldwide energy output (36.7% in 2019). In Malaysia, the major economies have boosted the quantity of coal-fired power plants necessary to sustain the requisite energy production (Khaw Lee Ping et al., 2022). The year 2021 was highlighted by the shortage of precipitation in a vast section of the Brazilian territory, which led to an energy catastrophe in the nation (Singh et al., 2022). Therefore, due to the massive production of the bottom ash, the materials were examined and proposed as suitable materials to improve the characteristics of the problematic soils via the ground improvement technique.

Bottom ash denotes the granular and incombustible residue of burned materials, for instance, coal, which is retrieved from the bottom of burners (Gencel et al., 2022). Bottom ash is claimed to form up to 21% of the overall residual residue on the burner after coal combustion (Ul Haq et al., 2014) having particles that vary from crude to delicate aggregate sizes (Singh & Siddique, 2015). This equates to 0.6–2.1 tons of bottom ash per kilowatt of electricity generation (Gencel et al., 2022). Even though the generated bottom ash can be grounded to provide an additional cementitious material (Choeycharoen et al., 2022), it may be utilized as a delicate aggregate to replace sand in traditional concrete (Khaw Lee Ping et al., 2022). According to Gencel et al., (2022), the physical materialization of coal bottom ash is comparable to river sand with greater friction durability and smaller total contraction than river sand. According to recent research made by Khaw Lee Ping et al., (2022), the bottom ash can bring value-added features to the present building sector, which will help both the economy and the environment.

Consequently, the environmental benefits of bottom ash when utilized as a replacement to the traditional delicate aggregates can be connected to the removal of the requirement to discard the bottom ash wastes in dumpsites paired with acting as an alternate supply for raw materials. The utilization of bottom ash in ground improvement as a green substitute for soft clay soils is obtaining considerable impetus, and there must subsist a thorough comprehension of the characteristics of bottom ash and its influence on the characteristics of problematic soils. Even though, there is a lot of research conducted related to the industrial waste, for instance, steel slag waste by Rezaei-Hosseiniabadi et al., (2022a) and Rezaei-Hosseiniabadi et al., (2022b), and identical observation on some parameters have been made

between this studies and the mentioned studies. However, a universal relationship via the statistical analysis has not been deeply explored, and there is no investigation on the utilization of bottom ash waste as granular columns to alter the characteristics of the problematic soils have been conducted. Thus, this paper focuses on the conception of the geotextiles-encased bottom ash column behavior under lateral loading via unconfined compression tests. Besides, this study also aimed to explore the function of the encapsulated bottom ash columns in enhancing the shear strength and compressibility and altering the engineering properties of the soft reconstituted kaolin clay. In addition, we hypothesized that (1) encapsulated bottom ash column may alter the physical and mechanical properties of the soft kaolin clay soils; (2) encapsulated bottom ash column may increase the shear strength of the soft kaolin clay soils with various dimensions; and (3) a prediction model to predict the shear strength may be developed based on the various independent variables. Thus, the objectives of the present study were to (1) establish the physical and mechanical characteristics of kaolin clay and bottom ash, (2) evaluate the undrained shear strength of the kaolin clay and kaolin clay reinforced with various dimensions of single and group of encapsulated bottom ash columns, (3) to formulate a regression correlation coefficient in proclaiming the effect of the encapsulated bottom ash column at various dimensions to the undrained shear strength of the soft kaolin clay soils.

Materials and methods

Materials

Figure 1 shows the location of the obtained material used in this study. As illustrated in the figure, the bottom ash was gathered from Tanjung Bin power plant in Johor ($1^{\circ} 19' 48''$ N, $103^{\circ} 32' 24''$ E) which is one of the four (4) coal power plants in Malaysia. Tanjung Bin is the largest coal-fired energy plant in Southeast Asia that is owned by Malakoff Corporation Berhad, based in Kuala Lumpur, Malaysia. The encapsulated bottom ash has a macro-porous material with sufficiently large pore dimensions. The bottom ash was ensconced in the soft clay utilizing the substitution technique. The sample of geotextile that was selected to encapsulate the soft clay reinforced with encapsulated bottom ash column was the polyester non-woven geotextile needle-punched fabric (MTS 130).

Kaolinite is a clay mineral with a chemical composition of $\text{Al}_2\text{Si}_2\text{O}_5(\text{OH})_4$ that stands for aluminum silicate hydroxide. It is easily broken especially when it is wet. It also owns a platy structure, which is hydrophilic, where it tends to mix or be wetted by water and form a slurry to produce homogeneous soft clay. The kaolin powder has a plate-like structure

and was bought from Kaolin (M) Sdn. Bhd ($4^{\circ} 9' 48.6''$ N, $101^{\circ} 16' 25.32''$ E) which is based in Selangor, Malaysia. Kaolin clay was prepared using the customized compaction method. Kaolin powder Grade S300 was used as the material to produce the repeatable homogeneous soft clay samples (see Table 1).

USCS unified soil classification system, *AASHTO* American Association of State Highway and Transportation Officials, *IMC* initial moisture content, *SG* specific gravity, *LL* liquid limit, *PL* plastic limit, *PI* plasticity index, *MDD* maximum dry density, *OMC* optimum moisture content, *UCS* unconfined compression strength, *USS* undrained shear strength

Experimental design

Sample preparation

The samples for the Atterberg limit test, particle size distribution test, compaction test, specific gravity test, permeability test, relative density test, unconfined compression (UCT) test, and unconsolidated undrained (UU) test were prepared according to the American Society of Testing and Materials (ASTM) and British standard as highlighted in Table 2. The density for the bottom ash columns for the UU test and UCT test was prepared uniformly by utilizing the same mass of bottom ash and the volume of the hole that was filled by the bottom ash. The samples for the UU and UCT tests were 50 mm in diameter and 100 mm in height, and the density obtained for every specimen was 0.9921 g/cm^3 . For the kaolin sample, the air-dried kaolin powder was mixed with 18.40% of water, which was the OMC of the kaolin obtained from the standard compaction test. The mass of kaolin in each specimen was fixed at 305.14 g to get the uniformity of all the specimens. After thoroughly mixing the soil, the wet soil was poured into the customized steel mold with 180-mm height and 50-mm internal diameter (Fig. 2) and compacted in three (3) layers, where each layer was compacted with five (5) free fall blows of 3.10-kg customized steel hammer. The customized mold shown in Fig. 2a was designed so that the amount of kaolin clay inside the specimen can be compressed into a 50-mm diameter and 100-mm height specimen.

In this research, the stone column diameter used was 0.6–1 m. The diameter of the bottom ash column in this study varied from 10 to 16 mm while the bottom ash particles used for laboratory tests were between 0.6- and 2.36-mm BS sieve. Bottom ash was poured into the split form mold, lined with double-layer rubber membranes, and fixed at the triaxial test apparatus. Since the bottom ash is a granular material, double-layer rubber membranes were used to avoid any leakage to occur. The bottom ash column model was constructed to support the layer of soil and to depict the condition in the



Fig. 1 Location of kaolin clay and bottom ash used in this study

construction field. This model was created to avoid the likelihood of the undulations of the soil, tilt, and uneven subsidence of the ground surface from the liquefaction of the underlying soil layers. The substitution technique was selected to eliminate the clay soil to produce an opening for the installation of the bottom ash column to minimize the disturbance in the soil and avoid heaving at the surface of the specimen from occurring. The opening for the bottom ash column installation was drilled by using drill bits at the desired diameter by using the replacement method.

Installation of bottom ash column

For kaolin samples reinforced with bottom ash columns, the procedure is identical to the unreinforced sample from the

mixing of the kaolin clay until the sample was compacted in three (3) layers with five (5) free fall blows using 3.10 kg of customized steel hammer. Additionally, when the samples were still inside the mold, the drill bits were used to drill the hole for the column in diameter either of 10 mm or 16 mm to prevent the specimen from expanding and extruded out of the mold and stored inside the particular case. The heights of the column were set to 60 mm and 80 mm in length for partially penetrating columns, and the height of the column of 100 mm in length was set for fully penetrating columns. For the next process, the specimens were extruded from the mold and stored in the particular case and were left for at least 24 h to let the pore water pressure stabilizes inside the specimen. The geotextile was used to encapsulate the bottom ash column to prevent excessive bulging. Geotextiles

Table 1 Engineering properties of soft kaolin clay soil

Properties	Unit	Result
Gravel	%	0
Sand	%	45
Clay and silt	%	55
USCS classification		ML
AASHTO classification		A-7-6b
IMC	%	0.96
SG		2.62
LL	%	41
PL	%	31
PI	%	10
MDD	g/cm ³	1.58
OMC	%	18.40
Coefficient of permeability	ms ⁻¹	2.5749 × 10 ⁻⁸
UCS	kPa	22.16
USS	kPa	11.08

were sewn to form cylinder-like geotextile mold to suit the diameter of the desired borehole and it was delicately placed inside the borehole. From the several results of the pilot test, the raining method has been decided for being the best way to create homogeneous bottom ash columns in kaolin clay specimens.

The bottom ash was densified by flowing it into the pre-drilled aperture by free fall where the falling height was set

at 10 mm from the tube to the surface of the clay specimen. The soft surface from the rear of the drill bit, utilized to drill an opening, was utilized to softly compress the bottom ash to prevent any voids from eventuating between the bottom ash. By applying this process, the disturbance of the soft kaolin clay specimen can be minimized. To sustain a uniform density in each bottom ash column, the mass of bottom ash was utilized to permeate the predrilled aperture based on the volume of predrilled aperture ash highlighted in Table 3. By using this method, the same density was produced for every specimen of the bottom ash column that was utilized to reinforce the kaolin clay.

Arrangement of pattern and size of encapsulated bottom ash column

There are two (2) dimensions of column utilized in this study: (1) using a single bottom column reinforced specimen which was inserted at the center of the specimens, and (2) a group of bottom columns-reinforced specimen with a triangular pattern. The triangular pattern was used to maintain the spacing between the columns installed. The interval between the columns was selected by examining the kaolin clay area ratio, and also the column area ratio for the whole clay area. This method was performed by positioning the columns to be in the center between the geometric centers of the kaolin samples to its border to transmit the load equally to each column. The column arrangement for single and

Table 2 Test standard and methods that are used for the main material

Material	Tests	Standard/method
Kaolin	Atterberg limit	
	- Liquid limit	BS 1377: Part 2: 1990: 4.3
	- Plastic limit	BS 1377: Part 2: 1990: 5.3
	Particle size distribution	
	- Sieve	BS 1377: Part 2: 1990: 9
	- Hydrometer	ASTM D 422: 1998
	Compaction	
	- Standard compaction	BS 1377: Part 4: 1990: 3.3
	Specific gravity	BS 1377: Part 2: 1990: 8
	Permeability	
Bottom ash	- Falling head	ASTM D 2434
	Particle size distribution	
	- Sieve	BS 1377: Part 2: 1990: 9
	Specific gravity	BS 1377: Part 2: 1990: 8
	Compaction	
	- Standard compaction	BS 1377: Part 4: 1990: 3.3
	Permeability	
	- Constant head	ASTM D 2434
	Relative density	BS 1377: Part 4: 1990: 4
	Kaolin (reinforced with encapsulated bottom ash columns)	Unconfined compression
Unconsolidated undrained triaxial		BS 1377: Part 7: 1990

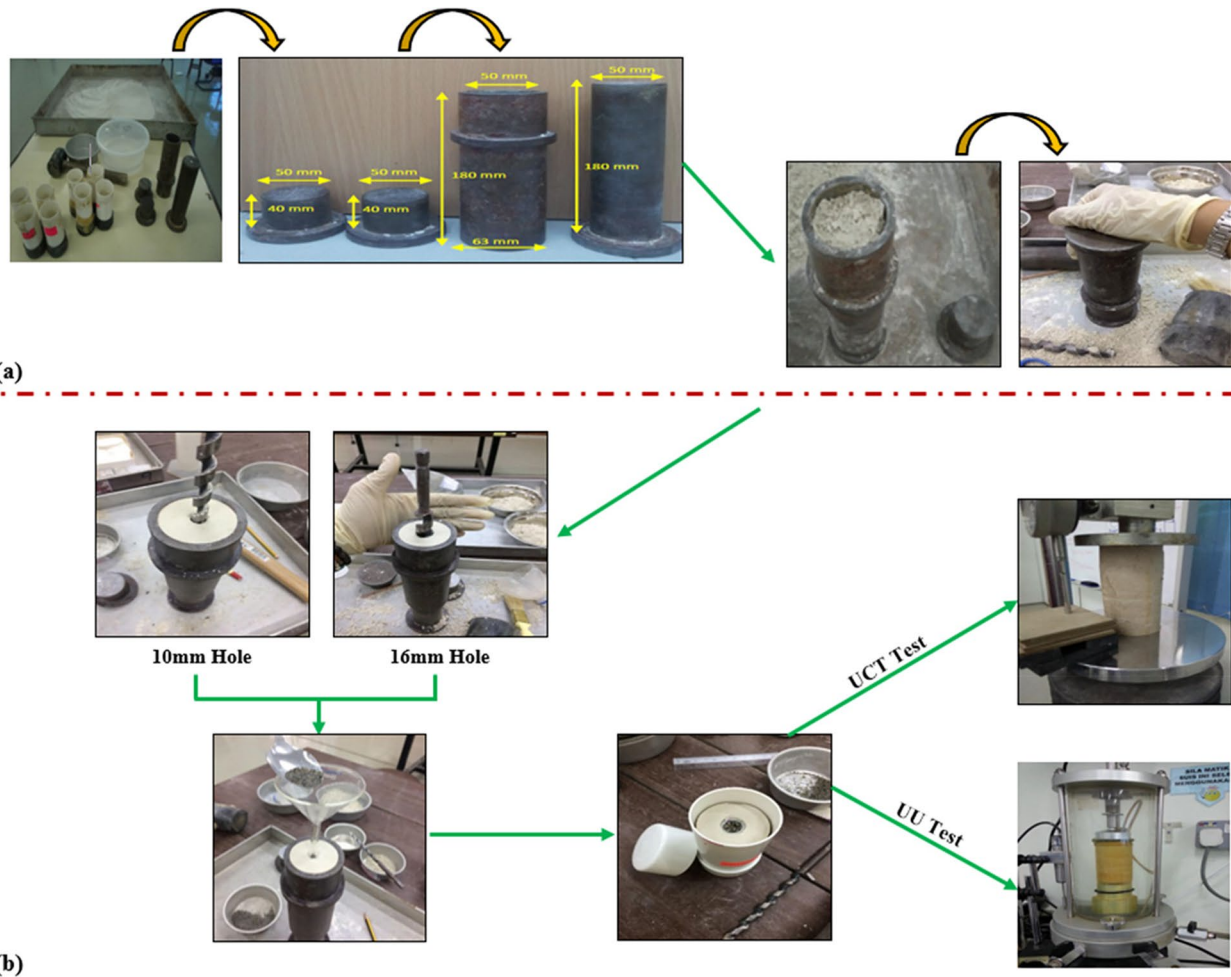


Fig. 2 Preparation of (a) kaolin sample and (b) kaolin reinforced with bottom ash column sample

Table 3 Density of bottom ash at various dimensions installed in kaolin specimens

Column diameter (mm)	Column length (mm)	Column volume with geotextiles (mm ³)	Density (g/cm ³)	Mass of bottom ash (g)
10	60	4712.39	0.5432	2.56
	80	6283.19		3.41
	100	7853.98		4.27
16	60	12,063.72		8.39
	80	16,084.95		11.19
	100	20106.19		13.99

group of encapsulated bottom ash columns installed in clay specimens was also measured according to the area replacement ratio (A_r), height penetrating ratio (H_p), height-diameter column ratio ($H-D_r$), and also volume penetrating ratio (V_r). The arrangement of single and grouped encapsulated bottom ash columns is illustrated in Fig. 3.

The width of the columns (D) and the particle size of granulated material (d) act as crucial parameters in

determining the suitable size of the column utilized in the prototype tests. Based on Muir-Wood et al., (2001), in the model tests, it is advisable to have a ratio of D/d to be equal to the prototype structures. In this research, the column width utilized was 10 and 16 mm, while the particle sizes of bottom ash were between 0.6 and 3.26 mm. Therefore, the value ratio D/d in this model test was between 4 and 17. Albeit the value of the lower range, D/d of prototype tests

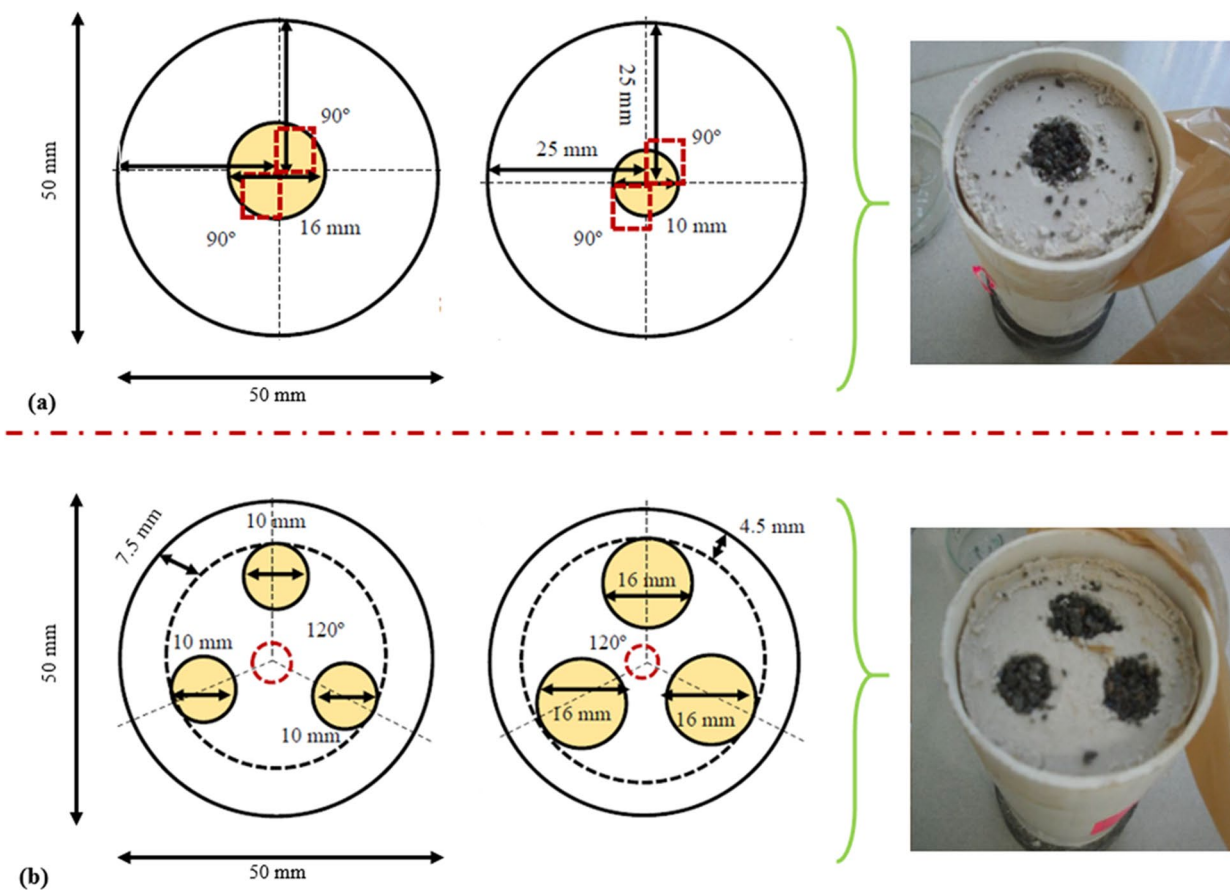


Fig. 3 Arrangement of (a) single and (b) grouped encapsulated bottom ash columns

was slightly lower than the ordinary in usage, it is unavoidable since there was a restriction on the width of the column to be utilized to evade border effects. The diameter of the bottom ash column in this test varied from 10 to 16 mm, and the ratio between the area of the column and the area of the specimen (A_r) which is known as the area ratio was 4% and 10.24% respectively. Whereas for group columns, the area ratio was 12% and 30.72% respectively. The height penetration ratio, which is defined as the ratio of the height of the column and the height of the specimen (H_p) varied from 0.6 to 0.8 for partially penetrating columns, and 1.0 for fully penetrating columns.

Determination of physical properties of the materials

There are four (4) physical properties investigated in this study which include particle size distribution, Atterberg limit, relative density, and specific gravity. The particle size distribution for fine-graded soil passing sieve size $63 \mu\text{m}$ was conducted in accordance with BS 1377: Part 2: 1990: 9 for sieve analysis and ASTM D 422: 1998 for hydrometer

analysis. The grain size distribution of fine soil, especially for particles that are finer than $63 \mu\text{m}$ was determined by conducting the hydrometer test. In this study, the sieves used for particle sizes of bottom ash were 20 mm, 10 mm, 4.75 mm, 2.36 mm, 1.18 mm, 0.6 mm, 0.3 mm, 0.15 mm, and 0.063 mm. The results of percentage passing versus sieve or particle size were plotted in the semi-logarithmic graph. The results of bottom ash were used to determine the similarity of the material with the group of soil in the classification system.

The plasticity ranges of clay soil can be measured in numerical expression by using Atterberg limits since the moisture content in clay soils was also known as plastic consistency. The test of kaolin clay was conducted by using the test method since the size range of their particles was finer than $63 \mu\text{m}$. The clay and soil tend to appear in four (4) states depending on certain moisture content, which is solid, semi-solid, plastic, and liquid. By using the cone penetration or the cone penetrometer method, the liquid limit test was conducted according to BS 1377: Part 2: 1990: Clause 4.3, while the plastic limit was conducted according to BS 1377: Part 2: 1990: Clause 5.3. The term plasticity index

(BS 1377: Part 2: 1990: Clause 5.4) comes from the numerical difference between the liquid limit and plastic limit.

The specific gravity of bottom ash and kaolin clay was determined by carrying out the small pycnometer test by referring to BS 1377: Part 2: 1990:8. The kaolin clay samples were put inside the small pycnometer, where the distilled water was already being filled half of the pycnometer which was then placed inside a vacuum chamber for 24 h. The air that existed in the sample that contained the distilled water and the mixture of the material was removed by the vacuum chamber. Then, the mass of the pycnometer was measured afterwards. The specific gravity is calculated by using Eq. 1.

$$G_s = \frac{m_2 - m_1}{(m_4 - m_1) - (m_3 - m_2)} \quad (1)$$

where m_1 is the mass of the empty pycnometer, m_2 is the mass of the pycnometer with dry soil, m_3 is the mass of the pycnometer with soil and water, m_4 is the mass of the pycnometer and water, and G_s is the specific gravity.

The relative density is conducted according to BS 1377: Part 4: 1990: 4. The gas jar method was selected for coarse grain material such as bottom ash (materials finer than 2.36 mm but coarser than 0.6 mm). The material was poured into a mold (with a predetermined volume), and the mass of the material was used to fill the mold and weighed afterwards. Therefore, the relative density of the bottom ash forming the vertical column was obtained by knowing the dry density of the bottom ash using Eq. 2.

$$D_r = \frac{\gamma_{\max}(\gamma - \gamma_{\min})}{\gamma(\gamma_{\max} - \gamma_{\min})} \times 100\% \quad (2)$$

where γ is the unit weight of the current sample, γ_{\min} is the minimum unit weight, γ_{\max} is the maximum unit weight and D_r is the relative density. Figure 4a shows the apparatus set up to determine the physical properties of the samples.

Determination of mechanical properties of the materials

In this study, there are two (2) mechanical properties explored thoroughly by means of compaction and permeability test. In order to determine the interconnection between the optimum moisture content (OMC) and the maximum dry density (MDD) for kaolin and bottom ash, the Standard Proctor compaction test was used in accordance with BS 1377: Part 4: 1990: 3.3 by utilizing a 2.5-kg hammer and 1-l capacity mold. Three (3) layers were compacted one by one by dropping the hammer via a free fall method with a distance of about 30 cm from the tip of the hammer to the soil with a total number of 25 blows per layer. The OMC and

MDD were determined from the graph plotted between the dry unit weights versus the moisture content.

The constant head test (ASTM D 2434) was utilized in determining the coefficient of permeability of bottom ash owing to the identical structure of bottom ash to the coarse grains. The samples were molded to form three (3) layers, where each layer was tamped with a total number of 27 blows. The coefficient of permeability can be determined after acquiring the data of water gathered at a certain time from the permeability test. The coefficient of permeability of kaolin was resolute by using the falling head test (ASTM D 2434). The permeameter of 8.2 cm in diameter was used to obtain the required data. Figure 4b illustrates the apparatus set up to determine the mechanical characteristics of the samples.

Determination of undrained shear strength of the materials

Determination of undrained shear strength of the materials used in this study was UCT and UU tests. The density of bottom ash for the specimen was 0.9921 g/cm³ while the sample of kaolin clay density was 0.1555 g/cm³. The density for both specimens was uniformly maintained in UCT and UU tests since the data need to be maintained for their uniformity.

The UCT was conducted according to the ASTM D 2166 to determine the strength of the soil since the unconfined compression imposed the axial loading without lateral confining pressure. In this test, the numerical data of axial load at failure and the corresponding axial strain were recorded. The test was prepared on the sample with an area replacement ratio of 4.00%, 10.24%, 12.00%, and 30.72%. Each sample of columns was installed with non-woven geotextiles and consisted of four (4) different height penetration ratios that were installed in kaolin which were 0, 60 mm, 80 mm, and 100 mm, and the controlled sample was used for the sample without any reinforcement of bottom ash columns. A total of 52 unconfined compression tests were conducted on the kaolin clay specimens as the test was conducted on 13 batches of sample, and each batch consisted of four (4) samples with different penetrations. The six (6) different types of non-woven geotextiles were encased for each sample with the same size of drifted holes. The outcome of the undrained shear strength acquired was half of the unconfined compressive strength. The undrained shear strength (S_u) of cohesive soil is equivalent to one-half the unconfined compressive strength (q_u) as shown in Eq. 3.

$$S_u = c = \frac{q_u}{2} \quad (3)$$

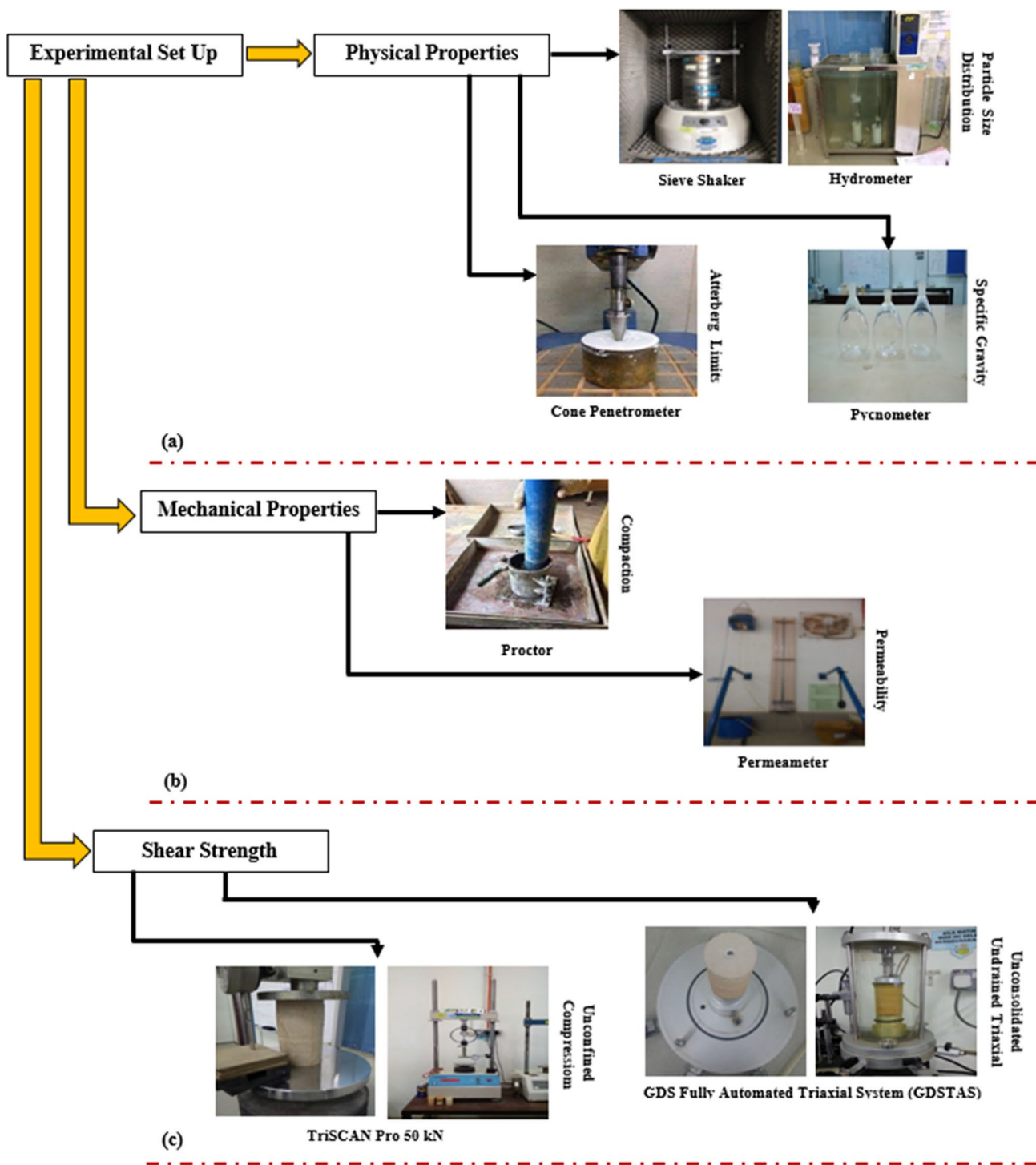


Fig. 4 Experimental set-up in determining (a) physical properties, (b) mechanical properties, and (3) shear strength

in which, S_u is the undrained shear strength, c is the cohesion, and q_u is the unconfined compressive strength.

The UU test was performed according to BS 1377: 1990: Part 7 to determine the shear stress and the total

stress of soft clay reinforced with single and group of encapsulated bottom ash columns. Four (4) different types of samples with different area replacement ratios of 4.00%, 10.24%, 12.00%, and 30.72% were prepared. Hence, a total

of 39 samples were prepared and tested. Table 4 shows the sample coding and testing program of UU triaxial tests for unreinforced clay and clay reinforced with encapsulated bottom ash columns.

The confining pressure was implemented to the sample via the chamber fluid, where the confining pressure, σ_3 is 70, 140, and 280 kPa. After a value of 20% strain was achieved, the chamber pressure was released and the water was emptied from the triaxial, the compression machine was inverted, the triaxial cell was lowered, and the machine was shut off. The sample was carefully eliminated and the entire equipment was dismantled. The shear strength of the kaolin reinforced with encapsulated bottom ash columns was calculated by using Eq. 4 to give the normal stress for the needed design.

$$\tau_f = c + \sigma \tan \phi \quad (4)$$

where c is the cohesion, σ is the sum of the normal stress, ϕ is the angle of internal friction, and τ_f is the shear strength. Figure 4c shows the apparatus set up to determine the undrained shear strength of the samples.

Statistical analysis

Numerical interpretations were performed through Microsoft Excel 2010. One-way analysis of variance (ANOVA) was conducted to collate the physical and mechanical

characteristics of the improved samples. Fisher's least significant difference (LSD) was employed to identify significant differences between means for different improvements at a level of $p < 0.05$. Furthermore, Pearson's correlation analysis was used to determine the correlations between the physical parameters that contributed to the improvement of the shear strength improvement. The error bars were used to indicate whether the results obtained for the samples are significantly different from each other. Regression analysis was used to develop an equation for prediction for shear strength improvements of the reinforced soft kaolin clay with encapsulated bottom ash in different variations of column dimensions based on Eq. 3.

$$y_i = \beta_0 + \beta_1 x_{i1} + \beta_2 x_{i2} + \dots + \beta_{p-1} x_{i,p-1} + \varepsilon \quad (5)$$

where y_i is the independent variable, x_i is the independent variable, β_0 is the intercept, $\beta_1, \beta_2, \dots, \beta_{p-1}$ are the coefficients of regression for the explanatory variables, and ε is the error term.

Results and discussion

Effects of encapsulated bottom ash column on the physical properties of soft kaolin clay

Figure 5a and b present the particle size distribution of kaolin and bottom ash samples respectively. Figure 5a

Table 4 Sample of coding and testing program of control and treated samples for UU tests

Sample	No. of column	Column dia. (mm)	Area ratio, Ac/As (%)	Area ratio, Ac/As with geotextile (%)	Column height (mm)	Column height penetrating ratio, Hc/Hs (%)	Column volume, (mm ³)	Volume penetrating ratio, Vc/Vs (%)
Control								
C	0	0	0	0	0	0	0	0
Single encapsulated bottom ash column								
S1060	1	10	4.00	2.19	60	0.6	2580.50	1.31
S1080	1	10	4.00	2.19	80	0.8	3440.67	1.75
S10100	1	10	4.00	2.19	100	1.0	4300.84	2.19
S1660	1	16	10.24	7.18	60	0.6	8461.57	4.31
S1680	1	16	10.24	7.18	80	0.8	11282.09	5.75
S16100	1	16	10.24	7.18	100	1.0	14102.61	7.18
Group of encapsulated bottom ash column								
G1060	3	10	12.00	6.57	60	0.6	7741.51	3.94
G1080	3	10	12.00	6.57	80	0.8	10322.02	5.26
G10100	3	10	12.00	6.57	100	1.0	12902.52	6.57
G1660	3	16	30.72	21.54	60	0.6	25384.70	12.93
G1680	3	16	30.72	21.54	80	0.8	33846.26	17.24
G16100	3	16	30.72	21.54	100	1.0	42307.82	21.55

C controlled sample, S1060 single encapsulated with column diameter of 10 mm and a column height of 60 mm, G1060 group of encapsulated with column diameter of 10 mm and a column height of 60 mm, Ac area of column, As area of sample, Hc height of column, Hs height of sample, Vc volume of column, Vs volume of sample

clearly shows that the kaolin sample resembles well-graded sand and the grain sizes range from clay to fine sand. The typical particle size distribution was obtained by plotting the graph between the percentage passing against the corresponding particle diameter. The majority size of kaolin clay was found to be in the range of 0.001–0.1 mm. Based on the AASHTO classification system, it can be deduced that kaolin clay can be classified as clayey soil (Group A-7-6b).

For the bottom ash (Fig. 5b), the particle size distribution was performed employing only sieve analysis following to dry sieving method since the particles of bottom ash are coarse in nature. A significant amount of particles falls within the range of 0.063–0.1 mm, which is in the sizes of fine sand to fine gravel. According to USCS and AASHTO, the bottom ash sample is categorized as well-graded sand (SW) and falls in the A-1 group and is labelled as A-1-a respectively. The findings of Muhardi et al., (2010) showed a C_u of 16.56 and a C_c of 1.01, making the bottom ash to be classified in identical categorization with the present study. Based on the plotted graph, the samples of bottom ash gradation portray identical trends and displayed well-graded size distribution which was also coherent with the results obtained by Hamada et. al., (2022). This has been certified by the value of the average coefficient of curvature and the average coefficient of uniformity, C_u obtained were 1.17 and 8.33 respectively. It can be deduced that the bottom ash in the Tanjung Bin power plant has a similar type of classification although the bottom ash has been generated in various kinds of batches of coal sources.

The Atterberg limit was conducted to kaolin clay only as the kaolin clay sample consists of finer particles coherent with the requirement stated in the standard and therefore this test was excluded for bottom ash samples. In this study, the

value of the liquid limit and plastic limit of kaolin clay was found to be 41% and 31% based on 20-mm penetration of the cone respectively with a plasticity index of 10%. Figure 6 shows the graph of penetration versus moisture content of liquid limit (Fig. 6a) together with the classification of kaolin clay based on the plasticity chart (Fig. 6b). As depicted in the plasticity chart, the kaolin S300 used in this study was located below A-line, and it has medium plasticity with a liquid limit obtained of 41% and a plasticity index of 10%. Thus, it is classified as ML (low plasticity silt).

The minimum and maximum densities for bottom ash obtained in the study were about 0.868 g/cm³ and 1.004 g/cm³ respectively which were used in bottom ash columns installation in kaolin samples. By using the raining technique, the average density of bottom ash based on the trial tests was about 0.9921 g/cm³. Thus, the relative density was determined as 92.34%. However, it is worth noting that the ability of the bottom ash column is not only for reinforcement but since the characteristic of the bottom ash column is quite similar to the vertical drain behavior, it has the potential to accelerate the dissipation of pore water pressure.

Based on the small pycnometer method, the specific gravity of kaolin was 2.62 while Tanjung Bin bottom ash was 2.33. The specific gravity of kaolin falls in a range of particle density of most soil. From previous research, Hasan et al., (2021b) reported that the specific gravity of kaolin was 2.64 while Tanjung Bin bottom ash was 2.35 (Hasan et al., 2011) which is a little higher than the current study. According to Head (1982), the specific gravity of most soils falls within a range of between 2.60 and 2.80. As the bottom ash was collected at different times, it was predicted that the specific gravity of bottom ash will be different because the properties of bottom ash in this power plant were not precisely identified from

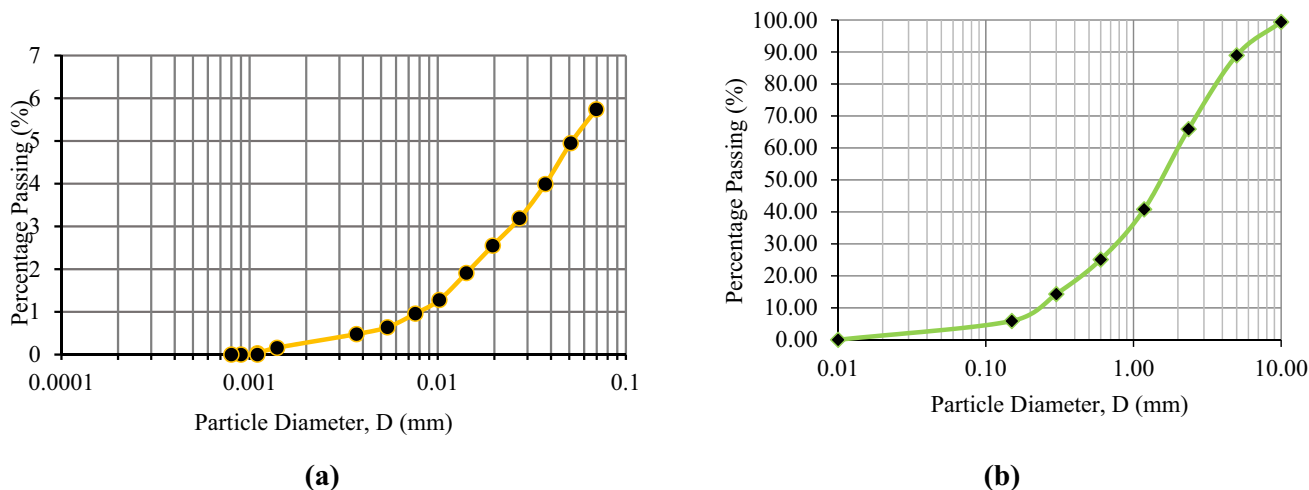


Fig. 5 Particle size distribution of (a) kaolin sample and (b) bottom ash sample

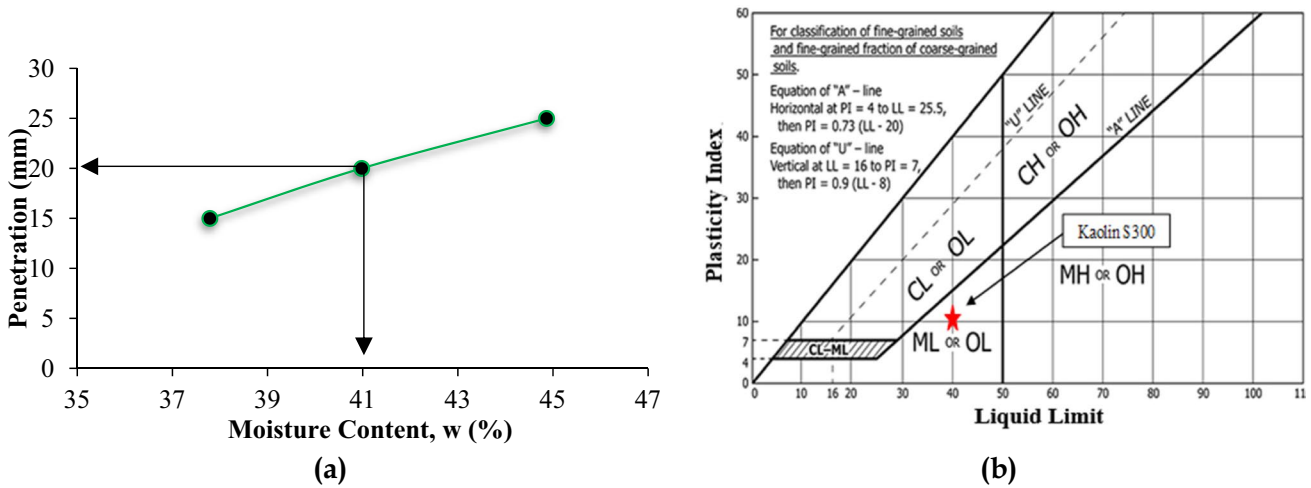


Fig. 6 Atterberg limits of kaolin sample. (a) Liquid limit of kaolin. (b) Classification of kaolin based on plasticity chart

time to time. According to Zaini et al., (2022a), the result of low specific gravity was due to high carbon content, while high iron content will create high specific gravity. The significant issue that caused the relatively low specific gravity was the low iron oxide content in the soil. The value of the specific gravity of bottom ash will determine the quality of bottom ash. As investigated by Kim et al., (2005) and Hasan et al., (2021a), the specific gravity which is low or lower than 1.6 indicates the low quality of the material and is attributed high percentage of porous texture and popcorn-like particles.

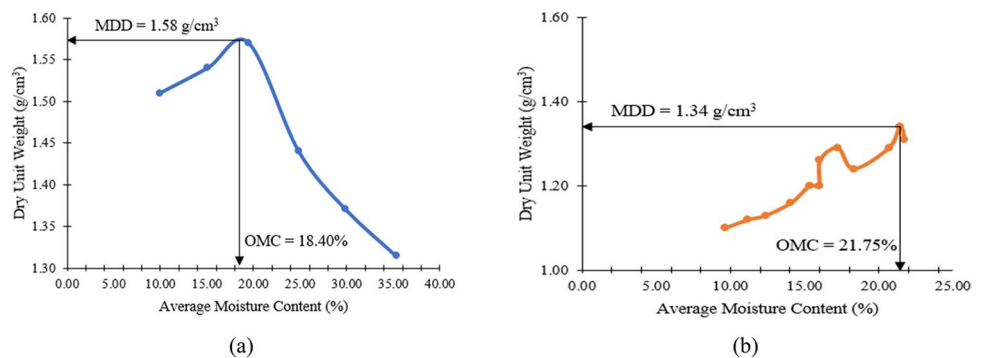
Effects of encapsulated bottom ash column on the mechanical properties of soft kaolin clay

Figure 7a and b show the relationship between the dry density and moisture content obtained from the compaction test for kaolin and bottom ash respectively. Based on the figure, the results show the MDD for kaolin obtained was 1.58 g/cm³ and OMC was 18.40% while, the MDD for bottom ash was 1.34 g/cm³ with an OMC of 21.75%. Based on the data obtained by Hasan et al., (2011), the values of MDD for

Tanjung Bin bottom ash were the same as in this study but quite different from OMC with a value of 23.5%. Compared to Muhardi et al., (2010), their result was not the same but was quantitatively similar with 1.31 g/cm³ of MDD and 21.5% of OMC. Muhardi et al., (2010) also reported that generally the compaction characteristics are affected by the low specific gravity and high air void content. Besides, the bottom ash was characterized as low density; thus, it was suitable to be constructed on a low-bearing capacity foundation like soft soils.

The value of the permeability coefficient of kaolin and bottom ash was obtained from the falling head and constant head tests. The coefficients of permeability for kaolin and bottom ash were 2.5749×10^{-8} m/s (at a dry density of 1.58 g/cm³) and 5.03×10^{-3} m/s (at a dry density of 1.34 g/cm³) respectively. Based on the results, the value coefficient of permeability for kaolin was much smaller compared to the value of bottom ash. As reported by Head (1982), it was expected for fine-grained clay soil, in which the kaolin possesses impermeable behavior and indicates poor drainage characteristics. The coefficient values of permeability obtained for bottom ash show that it has a

Fig. 7 Determination of MDD and OMC of (a) kaolin sample and (b) bottom ash sample



medium to a high degree of permeability, which represents a good drainage characteristic that is generally possessed by clean sand. The value in this study is quite higher and this is due to the higher MDD obtained. Compared to Muhardi et al., (2010), the coefficient of permeability was 1.72×10^{-4} m/s at the maximum dry density of 1.31 g/cm³. As reported by Hamada et al. (2022), the bottom ash which has fine particles tends to have a foremost effect on permeability that causes the permeability value to decrease as the fine particle increase.

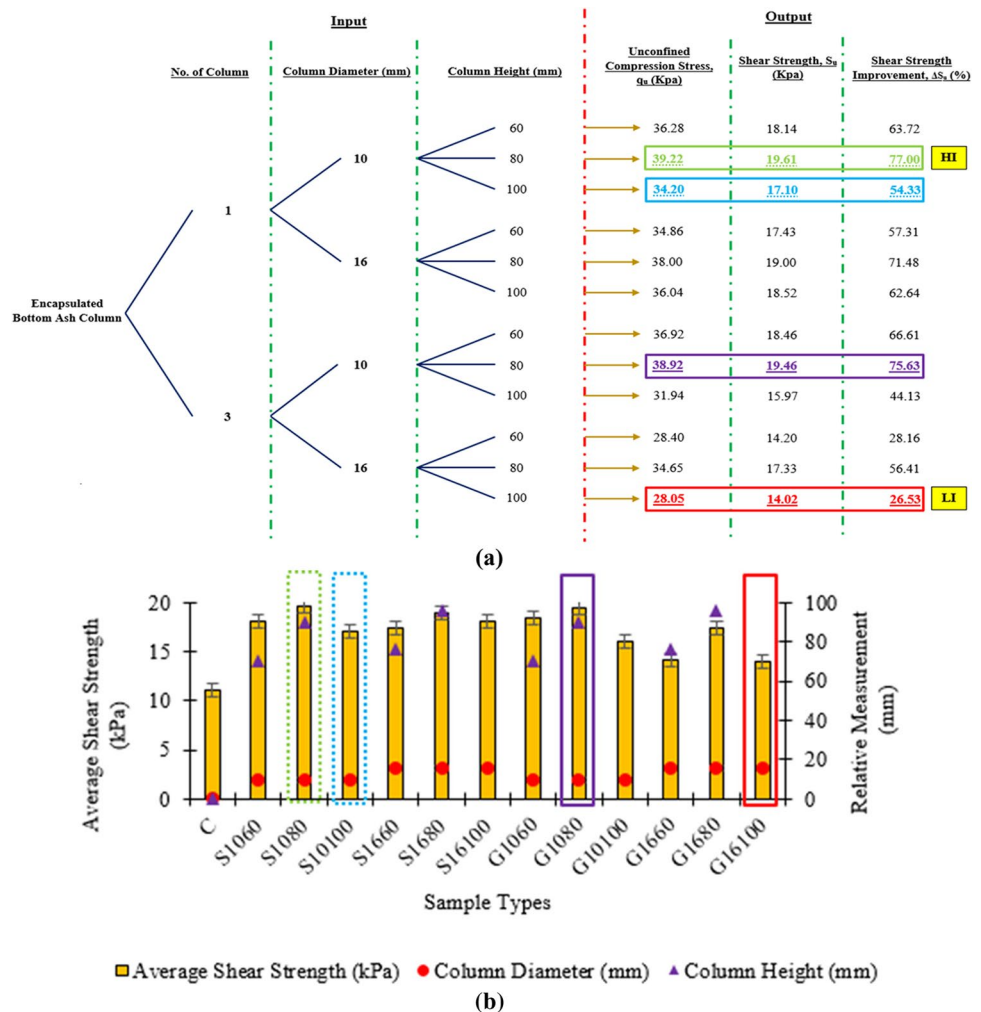
Effects of encapsulated bottom ash column installation on the shear strength of soft kaolin clay

Effects of encapsulated bottom ash column installation on the unconfined compressive strength

Figure 8a and b highlight the parameters involved with a percentage of shear strength improvement for the kaolin sample without any reinforcement and reinforced with single and group of encapsulated bottom ash columns. From

Fig. 8b, the average unconfined compressive strength for the five (5) controlled samples tested was 11.08 kPa. Meanwhile, in Fig. 8a, the average shear strength for clay samples reinforced with a single encapsulated 10-mm diameter of bottom ash column with 60.00%, 80.00%, and 100.00% of height penetrating column was 18.14 kPa, 19.61 kPa, and 17.10 kPa, with the improvement of shear strength of 63.72%, 77.00%, and 54.33%. In addition, when the kaolin samples were enforced with a single 16-mm column diameter with height penetrating columns of 60.00%, 80.00%, and 100.00%, the average shear strength of the samples was 17.43 kPa, 19.00 kPa, and 18.02 kPa respectively, which shows the improvement of shear strength of 57.31%, 71.48%, and 62.64% respectively. The largest enhancement of shear strength recorded for the single encapsulated column was 77.00% (denoted with a green box) with a column diameter and column height of 10 mm and 80 mm while the lowest shear strength improvement recorded for the single encapsulated bottom ash column was 54.33% (denoted with a blue box) with a 10 mm and 100 mm of column diameter and column height. At a 10-mm column diameter and a column

Fig. 8 Improvement of shear strength of kaolin clay reinforced with an encapsulated bottom ash column. Green box, highest shear strength improvement of single encapsulated bottom ash column; blue box, lowest shear strength improvement of single encapsulated bottom ash column; purple box, highest shear strength improvement of group encapsulated bottom ash column; red box, lowest shear strength improvement of group encapsulated bottom ash column; HI, highest improvement of reinforced kaolin clay; LI, lowest improvement of reinforced kaolin clay



height of 80 mm, the single encapsulated recorded the highest shear strength enhancement for all of the samples tested to enhance the shear strength of kaolin clay.

In this study, the triangular pattern was applied to kaolin clay samples reinforced with group encapsulated bottom ash. Based on Fig. 8, the average shear strength for 10-mm diameter of group encapsulated bottom ash columns with 60.00%, 80.00%, and 100.00% penetrating ratio was 18.46 kPa, 19.46 kPa, and 15.97 kPa with the shear strength improvement of 66.61%, 75.63%, and 44.13%. Meanwhile, for the group of three (3) 16-mm diameter columns with the height of penetration of 60.00%, 80.00%, and 100.00%, the average shear strength recorded was 14.20 kPa, 17.33 kPa, and 14.02 kPa with the percentage of improvement up to 28.16%, 56.41%, and 26.53%. The group encapsulated bottom ash columns with a column diameter and column height of 16 mm and 100 mm respectively recorded the lowest shear strength improvement (26.53%) for all of the samples tested in the study. Considering the performance of group encapsulated bottom ash columns using 10 mm and 16 mm of column diameter, the average shear strength raised until it reached the height penetrating ratio of 80% and then diminish when the height penetrating ratio was 100%. The undrained shear strength was intensified after the specimens had been strengthened by a single and a group of three (3) bottom ash columns. Based on the data obtained, the reinforcement increases the strength of the specimens for both single and group of encapsulated bottom ash columns. Based on the investigation, the geotextile encasement plays a crucial role in increasing the shear strength of the kaolin clay which led to strain hardening in the samples. Therefore, effectiveness of the increase in column diameter to improve the large displacement shear strength of the column-soil composites was more pronounce when the geotextile encasement was used which were in good agreement with those reported in the literature made by Rezaei-Hosseiniabadi et al., (2022a) and Rezaei-Hosseiniabadi et al. (2022b). The geotextile encasement binds the granular ash of the ground and makes the granular ash column of the ground function as a semi-rigid pile, which increases the cutting strength of the granular column-rock composite. The increase in the critical shear strength may be due to the developed tensile force in the geotextile process. The investigation made in this study is coherent to the studies conducted by Hasan et al., (2021b); the utilization of geotextile encasement does significantly increase the shear strength of the kaolin clay.

Effects of area replacement ratio (Ar) on the shear strength improvement of kaolin clay samples

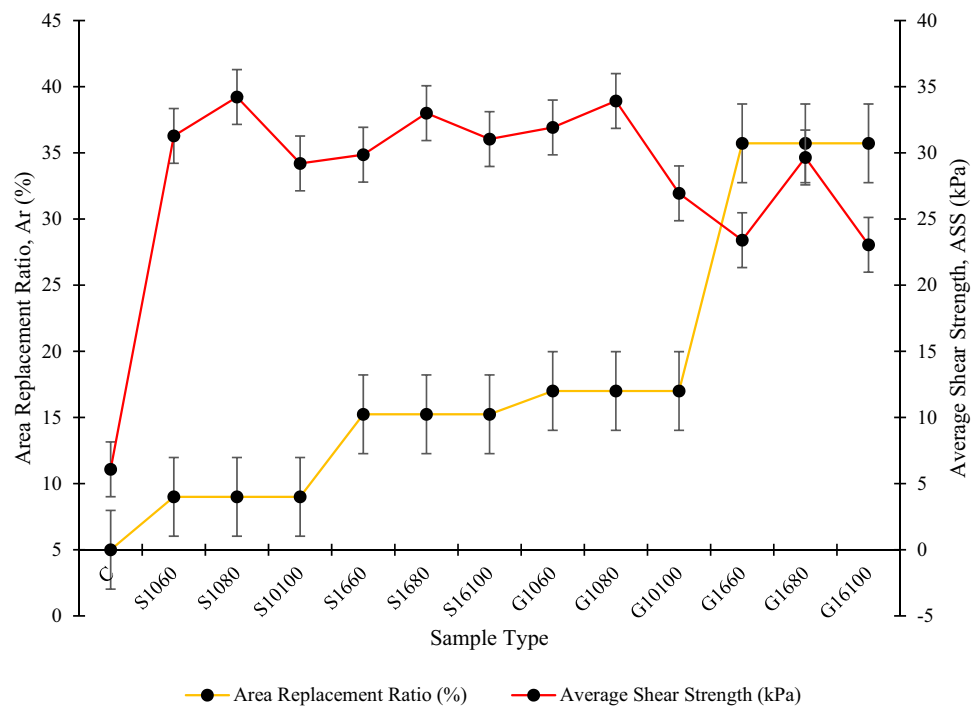
The effects of the replacement area ratio on the shear strength of the kaolin clays were investigated in this study. Figure 9 shows the interconnection between the area

replacement ratios, Ar, with the alterations on the shear strength of kaolin clay. Compared with the control sample, there is a significant improvement in shear strength of the kaolin clay when the sample was reinforced with single and group of encapsulated bottom ash columns at various area replacement ratios of 4.00%, 10.24%, 12.00%, and 30.72% from 11.08 kPa to the highest improvement of 39.22 kPa. In addition, the average shear strength of a single encapsulated bottom ash column with the Ar of 4.00% applicable for S1060, S1080, and S10100 (ASS = 36.57 kPa) was slightly greater compared to the Ar of single encapsulated bottom ash using 16-mm diameter column (Ar = 10.4%) resulted in S1660, S1680, and S16100 (ASS = 36.30 kPa) with a percentage difference of 0.74%.

Besides, the average shear strength of a group of encapsulated bottom ash column with the Ar of 12.00% applicable for G1060, G1080, and G10100 (ASS = 35.93 kPa) was slightly greater compared to the Ar of group of encapsulated bottom ash column using 16-mm diameter column (Ar = 10.4%) resulted in S1660, S1680, and S16100 (ASS = 30.36 kPa) with a percentage difference of 15.50%. Figure 9 clearly illustrates that the highest shear strength was recorded when the kaolin clay sample was reinforced with a single encapsulated bottom ash column at Ar = 4.00% (S1080). Coherent to that, the arrangement of single encapsulated bottom ash column (ASS = 36.43 kPa) resulted to higher average shear strength of kaolin clay when compared to a group of encapsulated bottom ash column (ASS = 33.15 kPa) with a percentage difference of 9.00%. Using granular columns proved that the Ar significantly influenced the degree of improvement in soft clay as reported by Hasan et al., (2021b), Rezaei-Hosseiniabadi et al., (2022a) and Rezaei-Hosseiniabadi et al., (2022b). The decrement in shear strength, at fully penetrating column, was due to a large portion of the soil was drilled and taken out from the specimen. Thus, it affected the natural state of the soil and will cause a reduction in the shear strength of the samples.

An investigation performed by Rezaei-Hosseiniabadi et al. (2022a), Rezaei-Hosseiniabadi et al., (2022b), and Tandel et al. (2012), stated that there was a decrease in performance due to the mobilization of larger confining stresses in the smaller column which was coherent with the results obtained in this study. The larger the confining stresses in the column, the larger the stiffness of the column with the smaller width. The shear strength for the group of encapsulated bottom ash column yielded a smaller improvement of shear strength owing to the large value of the area replacement ratio of the column which affects the surrounding column area. As the upright load was spread inside the column, the bulging occurred as the remaining width of the sample was too slender to grip the columns. The early shear strength of the soil reduced when a larger section of the soil was drilled from the specimen before the bottom ash was ensconced.

Fig. 9 Relationship between the area replacement ratio, Ar, with the shear strength of kaolin clay. ASS, average shear strength



Thus, the result suggested that the natural state of the soil was affected by the removed portion of the soil.

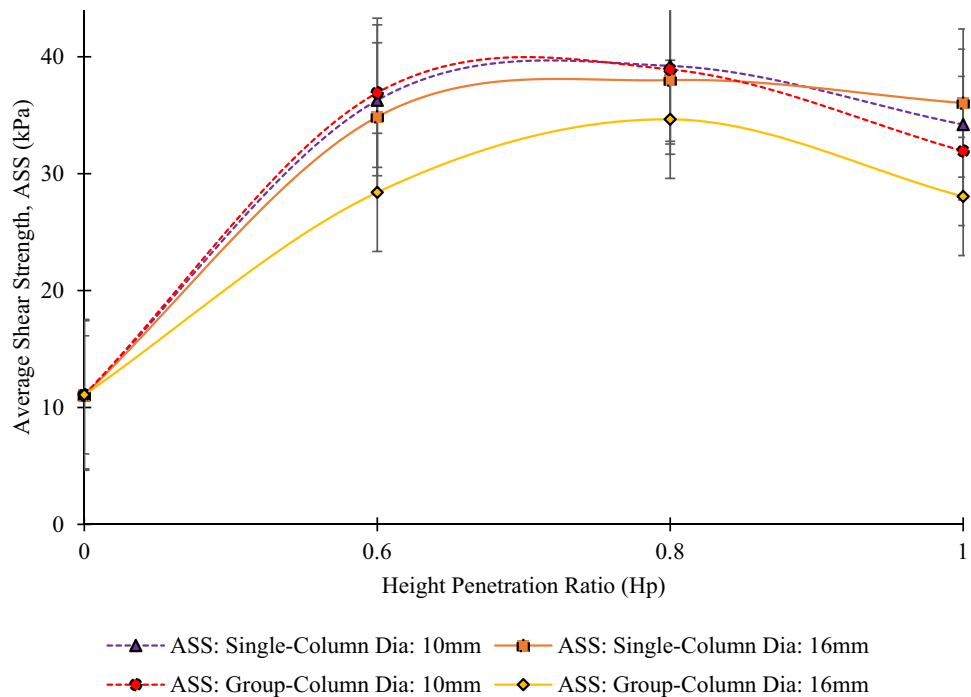
Effects of height penetration ratio (Hp) on the shear strength improvement of kaolin clay samples

The effects of Hp on the shear strength of the kaolin clays were examined in this study. Figure 10 shows the relationship between the height penetration ratios, Hp with the average shear strength of the kaolin clay reinforced with single encapsulated bottom ash column and group of encapsulated bottom ash column. Compared to the control sample, the reinforced kaolin clay with single and group of encapsulated bottom ash columns shows significant improvement of shear strength at the Hp of 0.6, 0.8, and 1.0 with a shear strength improvement from 11.08 to 36.28 kPa, and 34.68 kPa at Hp = 0.6, from 11.08 to 39.22 kPa and 38.00 kPa at Hp = 0.8, from 11.08 to 34.2 kPa and 36.04 kPa at Hp = 1.0 for a single encapsulated bottom ash column. Meanwhile, for a group of encapsulated bottom ash column, the shear strength improvement recorded was from 11.08 to 36.92 kPa and 28.4 kPa at Hp = 0.6, from 11.08 to 38.92 kPa and 34.65 kPa at Hp = 0.8, and from 11.08 to 31.94 kPa and 28.05 kPa at Hp = 1.0. For a single and group of encapsulated bottom ash columns, the highest improvement of shear strength fell at the Hp of 0.8, which remarks that the critical Hp is equal to 0.8 (see Fig. 10). Further increment in Hp more than 0.8 resulted to no increment in load carrying capacity. These results were supported by Hasan et al. (2011), who suggested that critical column length should be between 5 and 8 times

the width of the column, and the Hp acts as an important parameter in enhancing the improvement of undrained shear strength of the clay soil in comparison to the height over a diameter of the column ratio. The interaction between the individual bottom ash columns, the loaded area, and the surrounding soil can be comprehended as the behavior of piles with non-linear, sand-like axial stiffness properties as stated by Rezaei-Hosseiniabadi et al., (2022a), and Rezaei-Hosseiniabadi et al., (2022b). The column will permeate the underlying clay if the column is short for a substantial load to be conveyed to the bottom of the column. The penetration will be reduced if there is an increment in the column length because there will be fewer loads that transfer to the bottom of the column.

The behavior of the bottom ash column as a pile can be directly compared to this mode. The load transporting capacity of the bottom ash columns was subordinate to the undrained strength of the ambient soil but as for encased stone columns, the capacity of the column which was influenced by the strength of the surrounding soil gradually decreased as the stiffness of geotextile increased, which resulted in the decrease in the lateral bulging of the stone columns (Rezaei-Hosseiniabadi et al. 2022a; Rezaei-Hosseiniabadi et al. 2022b). The circulation of stresses encompassing the soil is reduced as there was an increment in the stiffness of geotextile and this will increase the stability of the column (Prasad & Satyanarayana, 2021). By encapsulating the column with geotextiles, a higher degree of compaction can be achieved, and it can help in enhancing the shear strength of the soil.

Fig. 10 Relationship between the height penetration ratios, H_p , with average shear strength of single and group of encapsulated bottom ash columns of kaolin clay. ASS, average shear strength



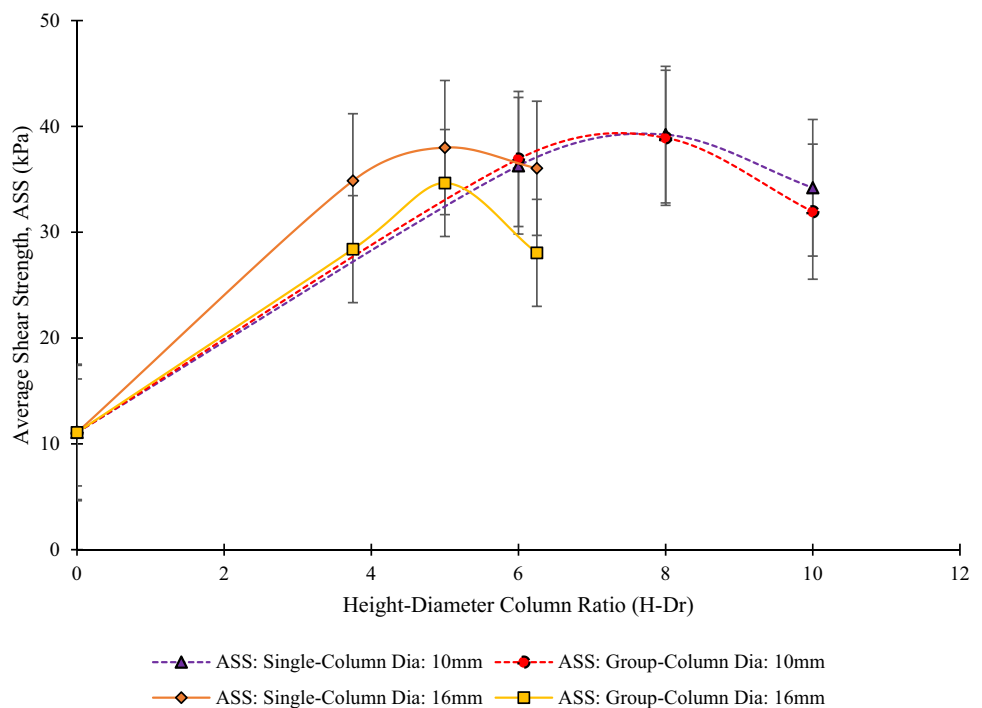
As clearly illustrated in Fig. 10, the shear strength of kaolin clay will increase as the H_p increases. Although there is an increment in the shear strength, however, the improvement of the shear strength does not merely dependent on the H_p of single and group of encapsulated bottom ash columns only. The portion of soft clay was substituted with stiffer material like bottom ash, and the columns were encased with geotextiles that help in drainage. Thus, the significant increment in the percentage of shear strength can be considered substantial as the penetration of single and group of encapsulated bottom ash columns was increased. The smaller diameter of encased bottom ash columns shows a better performance compared to the bottom ash column with a bigger diameter; this is owing to the mobilization of the larger confining stresses in the larger bottom ash columns which is coherent with the previous results obtained by Nagy (2013).

Effects of height-diameter of column ratio (H-Dr) on the shear strength improvement of kaolin clay samples

The effects of the height-diameter column ratio on the shear strength of the kaolin clay were investigated in this study. Figure 11 shows the relationship between the height-diameter column ratios, H-Dr, with average shear strength for kaolin clay reinforced with single and group of encapsulated bottom ash columns. The figure clearly illustrates that the highest shear strength of reinforced kaolin was recorded at the critical column length of 0.8 for all samples that were reinforced with single

and group of encapsulated bottom ash columns at the H-Dr of 8.0 (S1080 and G1080) and 5.0 (S1680) respectively with the average shear strength of 39.22 kPa, 38.92 kPa (for single encapsulated bottom ash column) and 38.00 kPa and 34.65 kPa (for group of encapsulated bottom ash column). The maximum improvement of shear strength for the reinforced kaolin clay was observed in S1080 with the average shear strength of 39.22 kPa at H-Dr = 8.0, and the lowest improvement of shear strength was observed in G16100 with the average shear strength of 28.05 kPa at H-Dr = 6.25. Besides, most of the kaolin clays reinforced with single encapsulated bottom ash column resulted to higher average shear strength compared to the kaolin clay reinforced with group of encapsulated bottom ash column as three (3) samples: G10100 (H-Dr = 10.00), G1660 (H-Dr = 3.75), and G16100 (H-Dr = 6.25) and were found to be at the lowest shear strength improvement with the average shear strength of 31.94 kPa, 28.40 kPa, and 28.05 kPa. The alteration of the column diameter and column height resulted to the variation of H-Dr value. Coherent to that, the increment in H-Dr does not result to the continuous increment in shear strength of the reinforced kaolin clay; however, the H-Dr value does affect the increment in the shear strength of the reinforced kaolin clay due to the interconnection of the H-Dr value with various column heights and column diameters. As what can be seen in Fig. 11, the highest shear strength was at the peak when H-Dr = 8.0, at critical column length of 10-mm diameter of single encapsulated bottom ash column. Further increment in H-Dr value resulted to the shear strength reduction of the reinforced kaolin clay.

Fig. 11 Relationship between the height-diameter column ratios, H-Dr, with average shear strength of single and group of encapsulated bottom ash columns of kaolin clay. ASS, average shear strength



The results obtained in the study were conformed to the outcomes obtained by Nagy (2013), Hasan et al., (2021b), Rezaei-Hosseinabadi et al., (2022a), and Rezaei-Hosseinabadi et al., (2022b) as the studies agreed that the highest improvement of shear strength occurred at the critical column length. The utilization of bottom ash columns in ground improvement in terms of H-Dr does influence the degree of shear strength improvement in kaolin clay as reported by Hasan et al., (2021b). The increase in the shear strength is due to the increased interconnection of the host soil and the granular column particles with the surface adhesive of the geotextile, which has improved the shear properties of the interface. Although there is an increment in the shear strength, however, the improvement of the shear strength does not merely depend on the H-Dr value of single and group of encapsulated bottom ash columns only. Besides, the decrement in shear strength at a fully penetrating column with a bigger diameter resulted to the large fraction of soil replaced by bottom ash particles. Thus, it affected the natural condition of the soil and causes a reduction in the shear strength of the samples due to the weak structure and the weak bonding particles of the sample.

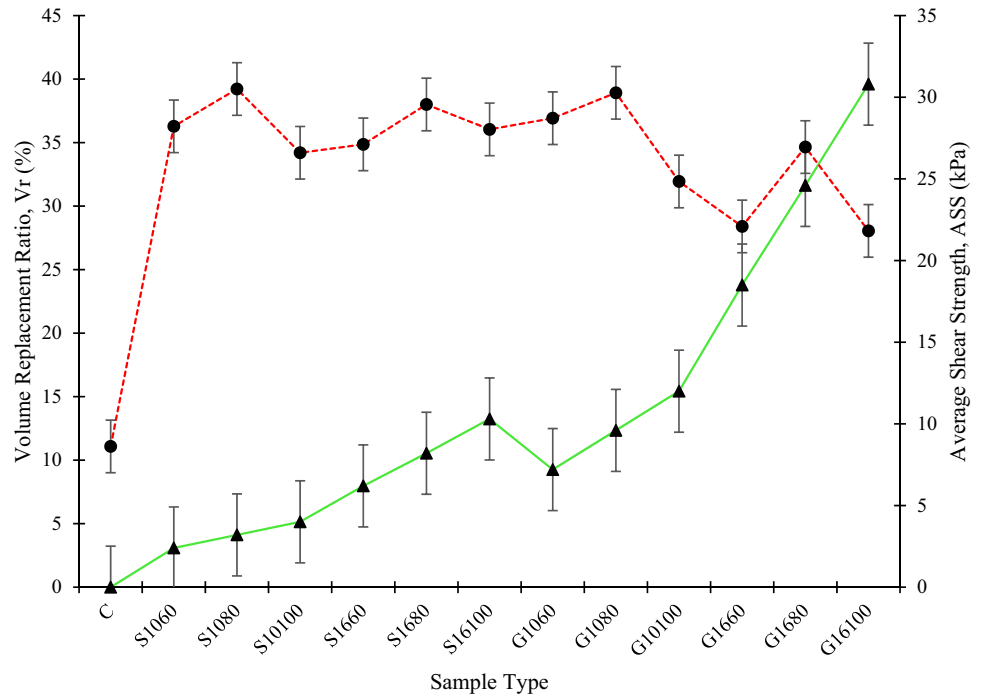
Effects of volume replacement ratio (Vr) on the shear strength improvement of kaolin clay samples

The effects of Vr on the shear strength of the kaolin clays were investigated in this study. Figure 12 shows the relationship between Vr and the average shear strength for kaolin clay reinforced with single and group of encapsulated bottom

ash columns. According to the illustrations, the installation of single and group of encapsulated bottom ash columns as kaolin clay reinforcement does improve the shear strength of the kaolin clay soil from 11.08 kPa to the maximum improvement of 39.22 kPa at all Vr value when compared to the control sample. Besides, the highest peak of Vr value (Vr = 30.8) illustrated in Fig. 12 does not result to the highest improvement of the shear strength as the shear strength at Vr = 30.8 is recorded at 28.05 kPa, and at the lowest peak of Vr (Vr = 2.4) does not result to the lowest improvement of the shear strength as the shear strength recorded is 36.28 kPa. Coherent to that, the highest peak of shear strength which resulted to the highest improvement of shear strength was examined when the bottom ash was utilized as single encapsulated bottom ash granular column at critical column height of 0.8 with a diameter column of 10 mm. Therefore, it can be validated that, the Vr value is directly proportional to the column diameter and column height. The increment in column height and column diameter resulted to the increment in Vr value. However, the increment in Vr value does not ensure continuous improvement in the shear strength of the reinforced soil as observed in Fig. 12 but does affect the performance of the reinforced encapsulated bottom ash column. If the soil expands, the particle density decreases, the strength decreases, and the sharp stress decreases. The stress-stress relationship decreases when the material stops expanding or contracting and breaks the interparticle bonds.

This study is coherent to the previous work done by Hasan et al., (2021b). The highest improvement of shear strength observed in the study was due to the small value

Fig. 12 Relationship between the volume replacement ratios, V_r , with average shear strength of single and group of encapsulated bottom ash columns of kaolin clay. ASS, average shear strength



of the area replacement ratio of the column which affects the surrounding column area. At this point, the interlocking between the particles and the bonding between the particle contacts are stronger as the kaolin clay was supported by the encapsulated bottom ash column. Moreover, the decreases in the performance of the bottom ash column were due to the mobilization of larger confining stresses in the smaller column which was coherent with the results obtained in this study. The larger the confining stresses in the column, the larger the stiffness of the column with the smaller width. The shear strength for the group of encapsulated bottom ash column yielded a smaller improvement of shear strength owing to the large value of the area replacement ratio of the column which affects the surrounding column area. As the upright load was spread inside the column, the bulging occurred as the remaining width of the sample was too slender to grip the columns. As the upright load was spread inside the column, the bulging occurred as the remaining width of the sample was too slender to grip the columns. Besides, the soil's shear resistance is the result of friction, particle interconnection, and particle contact linkage. Due to interlocking, the particle material may expand or contract in volume due to bending pressures. If the soil expands, the density of the particles decreases and the resistance decreases; in this case, the maximum resistance will be reduced as the shear stress decreases. When the material stops expanding or decreasing and the interparticle bonds break, the stress-stress relationship decreases. Volume change behavior and friction between particles depend on particle density and intergranular contact forces.

Effects of encapsulated bottom ash column installation on the cohesion and friction angle

The unconsolidated undrained (UU) test was conducted in determining the shear strength of soft clay reinforced with single and group of encapsulated bottom ash columns by examining three (3) samples of different penetrations with various confining pressures (70 kPa, 140 kPa, and 280 kPa). The effective shear stress parameters for the kaolin column reinforced with various diameters of the bottom ash column at various H_p , A_r , V_r , H -Dr, cohesion, and friction angle were investigated (see Table 5). The results show that the soft clay reinforced with encapsulated bottom ash column has higher effective cohesion compared to the control sample. Meanwhile, the effective friction angles show the slightest improvement since the difference with the control sample was quite similar. Generally, the improvement of reinforced soft clay with encapsulated bottom ash column can be discernable over the control sample.

The cohesion for the kaolin clay control sample was 13.9 kPa, and for the single 10-mm diameter column with a column height of 60 mm, 80 mm, and 100 mm were 15.0 kPa, 25.1 kPa, and 14.5 kPa respectively, while 22.0 kPa, 26.3 kPa, and 22.0 kPa respectively for the 16-mm column diameter. The cohesion value for the group column with a diameter of 10 mm and a column height of 60 mm, 80 mm, and 100 mm recorded a value of 19.1 kPa, 26.0 kPa, and 19.6 kPa respectively while for the 16-mm column diameter of the group of encapsulated bottom ash columns recorded a value of 18.9 kPa, 24.7 kPa, and 15.0

Table 5 Experimental value of shear strength, cohesion, and friction angle with respect to the eight physical parameters

No. of column	Cell pressure (kPa)	Column dia. (mm)	Column height (mm)	Ar	Vr	Hp	H-Dr	c (kPa)	Φ (°)
0	70	0	0	0	0	0	0	13.9	24.0
	140								
	280								
1	70	10	60	4.00	2.4	0.6	6	15.5	27.5
	140								
	280								
1	70	10	80	4.00	3.2	0.8	8	25.1	26.0
	140								
	280								
1	70	10	100	4.00	4.0	1.0	10	14.5	29.5
	140								
	280								
1	70	16	60	10.24	6.2	0.6	3.75	22.5	28.9
	140								
	280								
1	70	16	80	10.24	8.2	0.8	5	26.3	28.4
	140								
	280								
1	70	16	100	10.24	10.3	1.0	6.25	22.0	27.0
	140								
	280								
3	70	10	60	12.00	7.2	0.6	6	19.1	29.7
	140								
	280								
3	70	10	80	12.00	9.6	0.8	8	26.0	29.0
	140								
	280								
3	70	10	100	12.00	12.0	1.0	10	19.6	25.8
	140								
	280								
3	70	16	60	30.72	18.5	0.6	3.75	18.9	30.7
	140								
	280								
3	70	16	80	30.72	24.6	0.8	5	24.7	25.0
	140								
	280								
3	70	16	100	30.72	30.8	1.0	6.25	15.0	29.2
	140								
	280								

Ar area replacement ratio, Vr volume replacement ratio, Hp height penetration ratio, H-Dr height-diameter ratio, C_u undrained shear strength, C cohesion, Φ friction angle

kPa respectively. The highest cohesion value recorded in the study was at 26.3 kPa (S1680 sample) while the lowest value recorded for the cohesion was at 15.0 kPa (G16100 sample). The optimum cohesion value recorded for single and group of encapsulated bottom ash columns fell at 0.8 of Hp. Based on Table 5, the data validated that the higher value of confining pressure contributed to the

improvement of the cohesion value of improved samples compared to the control sample. There are significant differences in the cohesion value of the improved samples compared to the control sample as there is an increment in the cohesion value after the bottom ash column had been installed. Cohesion is the force that retains together particles within the soil (Zaini et al., 2022b). A higher cohesion

value will result in a higher bonding force between soil particles. As investigated by Rezaei-Hosseini et al. (2022b), there is a significant increase in the cohesion value when the samples were reinforced with the sand column. Therefore, the study proved that using the bottom ash column at various dimensions and arrangements can increase the cohesion value of the samples up to 26.3 kPa thus strengthening the bonding force between soil particles of the samples.

From Table 5, the friction angle, φ° of the control sample was recorded at 24.0. The friction angle for single and group of encapsulated bottom ash columns with a diameter of 10 mm and column height of 60 mm, 80 mm, and 100 mm were recorded at 27.5°, 26.0°, 29.5°, 29.7°, 29.0°, and 25.8° respectively. While for a column diameter of 16 mm for the single and group of encapsulated bottom ash columns with a height identical to a 10-mm diameter column, the friction angle was recorded at 28.9°, 28.4°, 27.0°, 30.7°, 25.0°, and 29.2°. The highest friction angle was recorded at 30.7° (G1660 sample) while the lowest friction angle was recorded at 25.0 (G1680 sample). The optimum friction angle recorded coherent to the highest shear strength improvement was at 26.0°. There are no significant differences in the friction angle of the improved samples when compared to the control sample as there is an increment in the friction angle after the bottom ash column had been installed. The friction angle for a given soil is the angle on the Mohr's circle of the shear stress and normal effective stresses at which shear failure occurs. Higher shear stress and normal effective stress will result in a higher friction angle. As verified by Frikha et al., (2015), the particle size of the column material had a tremendous effect on the behavior of reinforced clayey soil, including the rigidity, friction angle, and the characteristic of the shear strength. Hence, in this study, the bottom ash column installation at various dimensions and arrangements leads to higher shear stress and effective shear stress. The data validated that there is an effect on the friction angle when the shear stress and effective normal stress increase.

Stress-strain behavior

The shear stress-shear strain curves of the single and group of encapsulated bottom ash column-improved samples under confining pressures of 70 kPa, 140 kPa, and 280 kPa are illustrated in Fig. 13a to c. Results show that the shear stress of the single and group of encapsulated bottom ash samples at different column diameters and column heights increases with the increases in confining pressures. The increment of shear stress and axial stiffness of the specimen coherent with the eight (8) parameters studied can be clearly seen in the illustrated figure. For single encapsulated bottom ash column samples of 70 kPa, the highest improvement of shear stress was at 0.8 Hp value, due to the fact of critical column length proposed by

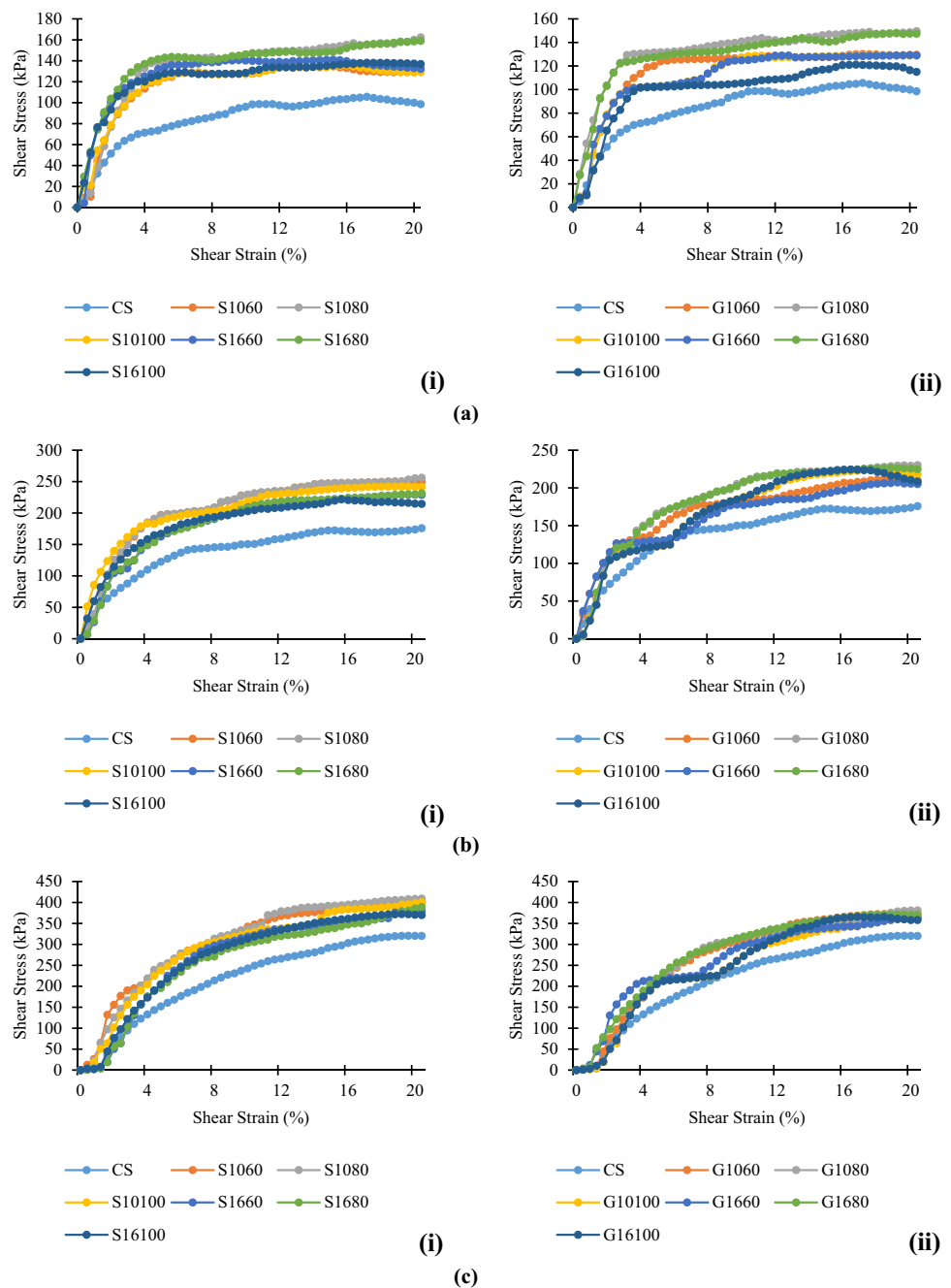
Najjar et al. (2010). The fully penetrating depth of the column at 100 mm resulted in the disturbance of the natural state of the soil since a large amount of kaolin clay have been removed from the samples. Thus, the shear strength of the kaolin clay will be reduced. Moreover, there would be insufficient depth to hold the specimen on a partially penetrating ratio of 0.6, where the stress is concentrated at the bottom of the specimen.

On the contrary, the single encapsulated bottom ash column samples with the confining pressure of 140 kPa had different kinds of patterns, where the highest improvement of deviator stress fell at 0.6 Hp. The lower shear stress also occurred due to the inequality of the shape of bottom ash particles and the arrangement of the bottom ash inside the geotextiles column. Besides, the single and group of samples with the confining pressure of 280 kPa resulted in the highest shear stress at 0.8 Hp. However, the improvement of shear stress at a 10-mm column diameter was higher compared to a 16-mm column diameter due to the smaller voids between the particles that present in a column diameter of 16 mm. Thus, the 16-mm column diameter has a huge tendency to experience disturbance and deformation compared to the 10-mm diameter column. This result coincided with the study made by Hasan et al. (2011), who proposed that the specimens reinforced with single bottom ash columns have the highest maximum deviator stress than the control specimens.

Based on Fig. 13a to c ii, at confining pressure of 70 kPa, the shear stress for both column diameters of 10 mm and 16 mm has the highest improvement at 0.8 Hp where the improvement was 49.01% and 39.93% respectively. While the shear stress at confining pressure of 140 kPa and 280 kPa for column diameters of 10 mm and 16 mm shows the same trends with the plotted shear stress of 70 kPa confining pressure where the highest improvement was recorded at 0.8 Hp with the improvement of 31.03%, 28.28%, 18.77%, and 15.64% respectively. Overall, for group encapsulated bottom ash column at 70 kPa, 140 kPa, and 280 kPa of confining pressure with 0.8 Hp shows an improvement in the shear stress compared to 1.0 Hp. Even though the Ar for the group column is higher, there is still an improvement in the 0.8 height penetrating ratio at the 10-mm diameter column, and this is due to the fact of a larger portion of soil is being replaced with the bottom ash column where it was three (3) times higher compared to the single column. The samples of fully penetrating column (1.0 Hp) with the highest Ar of 12.00 (10-mm diameter group column) and 30.72 (16-mm diameter group column) do not demonstrate the highest improvement of all the samples due to the large portion of kaolin clay specimens, which were removed, resulted to the disturbance on the structure of kaolin clay samples as the samples have high sensitiveness and tend to fail even before the bottom ash columns were ensconced.

Furthermore, the partially penetrating column at Hp of 0.8 of 70 kPa, 140 kPa, and 280 kPa confining pressures for

Fig. 13 Unconsolidated undrained triaxial test results for samples reinforced with encapsulated bottom ash column under various confining pressure of (a) at 70 kPa; (b) at 140 kPa; and (c) at 280 kPa. (i) Single encapsulated bottom ash column. (ii) Group encapsulated bottom ash column. CS, control sample; S, single encapsulated bottom ash column; G, group of encapsulated bottom ash column; column diameter: 10 mm and 16 mm; column height: 60 mm, 80 mm, and 100 mm



both column diameters of 10 mm and 16 mm showed more significant improvement in shear stress compared to the fully penetrating column due to a load of fully penetrating columns and was instantly enforced on the bottom ash columns at both ends, while a load of partially penetrating column was exposed directly only at the ends of bottom ash column, and as the other part was covered with clay. The risk of failure is quite high at a fully penetrating ratio since the column is longer. Thus, the bottom ash column tends to be crushed within the soil. Moreover, as stated by Wang et al., (2022), Rezaei-Hosseinabadi et al., (2022a), and Rezaei-Hosseinabadi

et al., (2022b), the improvement of load-carrying capacity will not participate in columns beyond the critical column length, and it was suggested that the column beyond the optimum length is more suitable in settlement design.

Statistical analysis and determination of the best regression model for shear strength improvement prediction via multiple regression analysis

The error bars indicate the standard error of the parameters observed in this study. The error bars were evaluated based

on the overlapping bars between the data and the length of the error bars within the same and different groups (at $p < 0.05$) of studies (see Figs. 8, 9, 10, 11, and 12) coherent to the studies made by Hasan et al., (2021a) and Zaini et al., (2022b). The overlapping error bars indicate the insignificant differences between the data while the data that is not overlapped indicates the significant differences in the data. Based on Fig. 8b, the mean shear strength of the improved kaolin clay by installing single and group of encapsulated bottom ash columns shows insignificant differences in value as the error bar overlapped with each other. However, the average shear strength of the improved kaolin clay and single and group of encapsulated bottom ash columns was significantly different from the control sample as the error bar does not overlap. Therefore, for Fig. 8b, a conclusion can be made validating that by implementing the bottom ash column at different column dimensions and arrangements can significantly increase the shear strength of the kaolin clay sample which is coherent with the laboratory data obtained. The error bars illustrated in Fig. 9 shows there are no significant differences between the improved kaolin clay encapsulated with single or group of bottom ash column but there are significant differences between the improved kaolin samples compared to the control sample at $p < 0.05$.

Based on Fig. 10, the results clearly conveyed the significant differences in the H_p between the single encapsulated bottom ash column with a column diameter of 10 mm and 16 mm and group of encapsulated bottom ash column with a column diameter of 10 mm with the group of encapsulated bottom ash column with a column diameter of 16 mm. Coherent to that, there are no significant differences in H_p value between the single encapsulated bottom ash column of diameter 10 mm and 16 mm and the group of encapsulated bottom ash column with a diameter of 10 mm. However, there are significant differences in the H_p value when compared to the group of encapsulated bottom ash column with a diameter of 16 mm. In Fig. 11, at $p < 0.05$, there are no significant differences between single and group of improved samples (10-mm and 16-mm column diameter) as the error bars do overlap with each other. Additionally, the length of the error bars is larger which resulted in the uncertain average value of the ASS. There are no significant differences between the single and group of 10-mm and 16-mm column diameter as the error bars for both of the samples do not overlap with each other. The error bars illustrated in Fig. 12 shows there are no significant differences in shear strength of the kaolin soil between the improved kaolin clay encapsulated with single or group bottom ash column but there are significant differences between the improved kaolin samples compared to the control sample at $p < 0.05$. The significant differences can be clearly seen in terms of V_r between the group of encapsulated bottom ash columns with 16-mm column diameter with the other reinforced kaolin clay.

The ANOVA test was performed to determine the statistically significant difference between the eight (8) parameters (no. of column, column diameter, column height, A_r , H_p , $H-Dr$, V_r , and confining pressures) observed in this study. Based on the one-way ANOVA, there is a significant difference between the eight (8) controlled parameters (at $p < 0.05$). Therefore, to specify which parameters contributed to the difference between the means, the Fisher's least significant difference (LSD) was performed as tabulated in Table 6 coherent with the one-way ANOVA conducted. There are 27 analyses conducted for the LSD; 14 analyses accepted the H_0 , while the other 13 analyses rejected the H_0 (accept the H_1 claim at average difference $> LSD$, where the $LSD = 14.74$). The analysis that contributed to the existence of the statistically significant difference is tabulated in Table 6. Based on the tabulated table, there is a significant differences between the numbers of column with the column diameter at a mean difference of 72.00, the numbers of column with the confining pressures at a mean difference of 161.49, the column diameter with the column height at a mean difference of 61.85, the column diameter with the confining pressures at a mean difference of 151.33, the column height with the A_r value at a mean difference of 60.70, the column height with the H_p value at a mean difference of 73.11, the column height with the $H-Dr$ value at a mean difference of 67.85, the column height with the V_r value at a mean difference of 63.31, the column height with the confining pressures at a mean difference of 89.49, the A_r value with the confining pressures at a mean difference of 150.59, the H_p value with the confining pressures at a mean difference of 162.59, the $H-Dr$ value with the confining pressures at a mean difference of 157.33, and the V_r value with the confining pressures at a mean difference of 152.79. The LSD was suggested by Xue et al. (2021) and Ai et al. (2021) for the mean separation.

Table 7 shows the Pearson's correlation coefficient performed to determine the correlation between the variables observed in this study. Ai et al., (2022) investigated that a correlation value which is below 0.4 is considered a weak correlation, above 0.4 is a strong correlation, and no correlation exists with the correlation value reaching 0. Based on the table, a strong correlation exists between the number of columns with the A_r and V_r with a correlation value of 0.76 and 0.72 respectively. Except for the confining pressures (almost no correlation exists), the correlation of column diameter, column height, H_p value, and $H-Dr$ value was weak due to the correlation value of less than 0.40. Four (4) parameters (column height, A_r value, H_p value, and V_r value) have a strong correlation with the column diameter and one (1) parameter ($H-Dr$ value) with a weak correlation with the column diameter. Besides, a perfect and very strong correlation existed between the column height with the H_p value and the $H-Dr$ value with a correlation value of 1.0 and

Table 6 Determination of specific parameters that contributed to the improvement of shear strength based on Fisher’s least significant difference

Mean	Absolute mean difference		Remark
	Mean diff.	Value	
\bar{x}_1	$\bar{x}_1-\bar{x}_3$	72.00	Difference is significant at $p= 0.05$, $LSD = 14.74$
	$\bar{x}_1-\bar{x}_8$	161.49	
\bar{x}_2	$\bar{x}_2-\bar{x}_3$	61.85	
	$\bar{x}_2-\bar{x}_8$	151.33	
\bar{x}_3	$\bar{x}_3-\bar{x}_4$	60.70	
	$\bar{x}_3-\bar{x}_5$	73.11	
	$\bar{x}_3-\bar{x}_6$	67.85	
	$\bar{x}_3-\bar{x}_7$	63.31	
$\bar{x}_3-\bar{x}_8$	89.49		
\bar{x}_4	$\bar{x}_4-\bar{x}_8$	150.19	
\bar{x}_5	$\bar{x}_5-\bar{x}_8$	162.59	
\bar{x}_6	$\bar{x}_6-\bar{x}_8$	157.33	
\bar{x}_7	$\bar{x}_7-\bar{x}_8$	152.79	

\bar{x}_1 number of column, \bar{x}_2 column diameter, \bar{x}_3 column height, \bar{x}_4 area replacement ratio (Ar), \bar{x}_5 height penetration ratio (Hp), \bar{x}_6 height-diameter column ratio (H-Dr), \bar{x}_7 volume replacement ratio (Vr), \bar{x}_8 confining pressure

0.83 respectively. The other two (2) parameters (Ar value and Vr value) show a moderately strong and weak correlation with the column heights. Moreover, with a correlation value of 0.95, the Ar value and the Vr value are strongly correlated with each other. A weak correlation exists between the Ar values with the Hp value ($r = 0.30$). There is a strong correlation that exists between the Hp values with the H-Dr value ($r = 0.83$) and the Vr value ($r = 0.43$). Table 7 shows that there is no correlation exist between the seven (7) parameters (number of column, column diameter, column height, Ar value, Hp value, H-Dr value, and Vr value) with the confining pressure as the correlation value is zero (column height only) and reaching zero.

The multiple regression analysis was performed to determine a specific mathematical equation and model to describe the relationship between the eight (8) controlled variables (number of column, column diameter, column height, Ar value, Hp value, H-Dr value, Vr value, and confining

pressures) with the shear strength. A prediction model was developed to predict the shear strength value (see Table 8), and the best prediction model was selected appropriate to the multiple regression analysis that contributed to the highest value of adjusted R^2 to predict the shear strength of the kaolin clay sample. In the study, there are a total of 93 analyses performed based on regression analysis. From the 93 analyses performed, 64 analyses were eliminated due to the value of adjusted R^2 lower than 0.2 which indicates a weak correlation between the variables analyzed, and the other 29 analyses were selected and tabulated in Table 8 based on the R^2 value which contributed to the strongest correlation between the variables studied.

Based on Table 8, the F -significant value for all of the regression equations rejected the H_0 at $p < 0.05$ which indicates that all of the equation is a good equations formulated for the regression analysis. Based on the equation, there are about more than 96.00% of the data

Table 7 Determination of the relationship between eight (8) controlled parameters studied according to Pearson’s correlation coefficient

Parameter	A	B	C	Ar	Hp	H-Dr	Vr	D
A	1.00							
B	0.37	1.00						
C	0.39	0.62	1.00					
Ar	0.76	0.66	0.30	1.00				
Hp	0.39	0.62	1.00	0.30	1.00			
H-Dr	0.32	0.16	0.83	0.077	0.83	1.00		
Vr	0.72	0.62	0.43	0.95	0.43	0.039	1.00	
D	7.6×10^{-18}	2.2×10^{-17}	0	1.3×10^{-17}	3.9×10^{-18}	1.7×10^{-17}	1.5×10^{-17}	1.00

A number of column, B column diameter, C column height, D confining pressure, Ar area replacement ratio, Hp height penetration ratio, H-Dr height-diameter column ratio, Vr volume replacement ratio

can be best explained by each of the models tabulated in Table 8. Therefore, a further analysis was performed to choose the best model for the shear strength prediction. Based on the adjusted R^2 value, the best prediction model that can be used to predict the shear strength in this study is as follows:

$$C_u = 17.02 - 2.790x_1 + 0.3352x_2 + 0.2069x_3 + 0.5649x_8 \tag{6}$$

where C_u is the undrained shear strength, x_1 is the number of columns, x_2 is the column diameter, x_3 is the column height, and x_8 is the confining pressures. Based on Eq. 4, it can be said that the undrained shear strength is strongly affected by the number of columns, column diameter, columns height, and different confining pressures. The adjusted R^2 for this equation is 0.9773 which

indicates that 97.73% of the data can be best explained by this model. Therefore, a conclusion can be made based on this model stating that the changes in the number of columns, column diameter, and column height are directly proportional to the changes in Ar value, Hp value, H-Dr value, Vr value, and the shear strength, while the confining pressures are directly proportional to the increment in the undrained shear strength value.

Conclusions

This study investigated the influence of encapsulated bottom ash column on the strength improvement of the soft kaolin clay. Based on the study conducted, the conclusions can be drawn as follows:

Table 8 Determination of the best regression model for shear strength prediction based on regression analysis

Regression equation	F-sig.	R^2	Adjusted R^2
$C_u = 31.17 + 0.5649x_8$	9.15×10^{-28}	0.9615	0.9604
$C_u = 31.78 - 0.3306x_1 + 0.5649x_8$	3.43×10^{-26}	0.9615	0.9594
$C_u = 21.16 + 0.8338x_2 + 0.5649x_8$	2.10×10^{-27}	0.9671	0.9652
$C_u = 16.62 + 0.1970x_3 + 0.5649x_8$	9.78×10^{-29}	0.9722	0.9707
$C_u = 32.74 - 0.12x_4 + 0.5649x_8$	2.64×10^{-26}	0.9621	0.9600
$C_u = 16.62 + 19.70x_5 + 0.5649x_8$	9.78×10^{-29}	0.9722	0.9707
$C_u = 18.50 + 2.111x_6 + 0.5649x_8$	4.38×10^{-29}	0.9734	0.9720
$C_u = 32.56 - 0.1325x_7 + 0.5649x_8$	2.74×10^{-26}	0.9620	0.9599
$C_u = 22.57 - 1.865x_1 + 1.003x_2 + 0.5649x_8$	2.53×10^{-26}	0.9685	0.9658
$C_u = 15.82 + 0.1907x_2 + 0.1769x_3 + 0.5649x_8$	2.49×10^{-27}	0.9724	0.9700
$C_u = 17.99 + 0.2312x_3 - 0.2961x_4 + 0.5649x_8$	2.94×10^{-28}	0.9756	0.9735
$C_u = 17.99 + 0.2312x_3 - 0.2961x_4 + 0.5649x_8$	3.60×10^{-29}	0.9756	0.9449
$C_u = 17.99 - 0.2961x_4 + 23.115x_5 + 0.5649x_8$	2.94×10^{-28}	0.9756	0.9735
$C_u = 16.62 + 7.983x_5 + 1.441x_6 + 0.5649x_8$	8.79×10^{-28}	0.9740	0.9718
$C_u = 20.04 + 2.131x_6 - 0.1574x_7 + 0.5649x_8$	7.80×10^{-28}	0.9742	0.9719
$C_u = 17.02 - 2.790x_1 + 0.3352x_2 + 0.2069x_3 + 0.5649x_8$	7.60×10^{-27}	0.9754	0.9725
$C_u = 14.27 + 1.172x_2 + 0.1382x_3 - 0.5614x_4 + 0.5649x_8$	3.04×10^{-28}	0.9797	0.9773
$C_u = 14.27 + 1.172x_2 + 0.1382x_3 - 0.5614x_4 + 0.5649x_8$	1.10×10^{-28}	0.9797	0.9479
$C_u = 17.82 + 0.1943x_3 - 0.2602x_4 + 0.4023x_6 + 0.5649x_8$	2.19×10^{-27}	0.9757	0.9434
$C_u = 17.82 - 0.2602x_4 + 19.43x_5 + 0.4023x_6 + 0.5649x_8$	6.53×10^{-27}	0.9757	0.9728
$C_u = 16.63 + 29.43x_5 - 0.2893x_6 - 0.5176x_7 + 0.5649x_8$	1.23×10^{-27}	0.9779	0.9755
$C_u = 12.82 + 2.016x_1 + 1.438x_2 + 0.102x_3 - 0.7733x_4 + 0.5649x_8$	4.20×10^{-27}	0.9802	0.9772
$C_u = 12.82 + 2.016x_1 + 1.438x_2 + 0.1019x_3 - 0.7733x_4 + 0.5649x_8$	2.85×10^{-27}	0.9802	0.9469
$C_u = 8.89 - 5.108x_1 + 3.372x_2 - 0.8423x_3 - 0.6887x_7 + 0.5649x_8$	3.28×10^{-27}	0.9870	0.9519
$C_u = 8.72 + 2.382x_2 - 0.3391x_3 - 0.4633x_4 + 4.165x_6 + 0.5649x_8$	4.02×10^{-29}	0.9848	0.9522
$C_u = 12.96 + 0.3395x_3 + 0.7945x_4 - 0.3025x_6 - 1.47x_7 + 0.5649x_8$	3.15×10^{-27}	0.9801	0.9468
$C_u = 12.96 + 0.7945x_4 + 33.95x_5 - 0.3025x_6 - 1.47x_7 + 0.5649x_8$	4.66×10^{-27}	0.9801	0.9771
$C_u = 9.11 - 4.723x_1 + 2.414x_2 - 0.5126x_3 + 0.0862x_4 + 6.422x_7 + 0.5649x_8$	2.61×10^{-28}	0.9864	0.9525
$C_u = 8.52 + 3.157x_2 - 0.5948x_3 - 1.13x_4 + 5.788x_6 + 0.8343x_7 + 0.5649x_8$	8.20×10^{-28}	0.9853	0.9513

C_u undrained shear strength, F -sig F -test, R^2 correlation of determination, x_1 number of columns, x_2 column diameter, x_3 column height, x_4 area replacement ratio (Ar), x_5 height penetration ratio (Hp), x_6 height-diameter column ratio (H-Dr), x_7 volume replacement ratio, x_8 confining pressure

- a) Kaolin clay can be categorized as ML, which indicates as low plasticity silt or inorganic silt of medium compressibility with a permeability value of 2.5749×10^{-8} m/s with a liquid limit (LL) of 41%, plastic limit (PL) of 31%, and plasticity index (PI) of 10% with a specific gravity of 2.62. In addition, based on the compaction test, the MDD of kaolin was 1.58 g/cm^3 with an OMC of 18.40%. The bottom ash falls in category A-1-a group which predominantly contains stone fragments with and without a well-graded binder of fine material and was classified as well-graded sand (SW) with a specific gravity of 2.33. The MDD of the bottom ash was 1.34 g/cm^3 with an OMC of 21.75%. Meanwhile, the permeability coefficient of bottom ash was 5.03×10^{-3} m/s (good drainage characteristic).
- b) The shear strength of the soft clay was significantly enhanced by installing the encapsulated bottom ash columns. The Ar and Hp have a great influence in improving the undrained shear strength of reconstituted soft clay reinforced with encapsulated bottom ash columns up to 77% of USS improvement. The highest improvement of shear strength was observed when 10-mm and 16-mm column diameter for both single and group of encapsulated bottom ash columns was utilized at 0.8 of Hp (critical column length). Further modification in Hp leads to decrement in the USS from 19.61 to 17.10 kPa (12.80% strength reduction) in single encapsulated bottom ash column with 10-mm column diameter, from 19.00 to 18.02 kPa (5.16% strength reduction) in single encapsulated bottom ash column with 16-mm column diameter, from 19.46 to 15.97 kPa (17.93% strength reduction) in group of encapsulated bottom ash column with 10-mm column diameter, and from 17.33 to 15.97 kPa (7.85% strength reduction) in group of encapsulated bottom ash column with 16-mm column diameter. Besides, the confining pressure plays a crucial role in the compressibility and shear strength of the soft clay reinforced with encapsulated bottom ash columns. The clogging situations that happened between the clay and the bottom ash columns have resulted in insufficient excess pore water to disperse well from the clay specimens. The results have confirmed that the installation of encapsulated bottom ash columns does alter the cohesion c , and the friction angle ϕ , and the strength and compressibility of kaolin clay samples from 13.9 kPa and 24.0° up to the highest improvement of 26.3 kPa and 30.7° observed in single encapsulated bottom ash column with 16-mm column diameter and group encapsulated bottom ash column with 16-mm column diameter.
- c) Based on the error bars plotted, compared to the control sample, the single and group of encapsulated bottom ash columns at different dimensions and arrangements do have significant effects on the

average shear strength of the kaolin clay at $p < 0.05$. Based on the one-way ANOVA, there is a significant difference between the eight (8) controlled parameters (at $p < 0.05$). Therefore, the Fisher's least significant difference (LSD) was performed to specify which parameters contributed to the difference between the means coherent with the one-way ANOVA conducted. There are 13 analyses accept the H_1 claim at average difference $> \text{LSD}$, where the $\text{LSD} = 14.74$. There is a significant difference between the numbers of column with the column diameter at a mean difference of 72.00, the numbers of column with the confining pressures at a mean difference of 161.49, the column diameter with the column height at a mean difference of 61.85, the column diameter with the confining pressures at a mean difference of 151.33, the column height with the Ar value at a mean difference of 60.70, the column height with the Hp value at a mean difference of 73.11, the column height with the H-Dr value at a mean difference of 67.85, the column height with the Vr value at a mean difference of 63.31, the column height with the confining pressures at a mean difference of 89.49, the Ar value with the confining pressures at a mean difference of 150.59, the Hp value with the confining pressures at a mean difference of 162.59, the H-Dr value with the confining pressures at a mean difference of 157.33, and the Vr value with the confining pressures at a mean difference of 152.79. Moreover, Pearson's correlation coefficient proved the relationship between the eight (8) independent parameters controlled in this study for at least one (1) variable having a strong correlation value above 0.4. Besides, based on the multiple regression analysis, 29 analyses that contributed to the good prediction model and the best prediction model was developed as shown in Eq. (4) with the adjusted R^2 value of 0.9773. Based on Eq. (4), 97.73% of the data can be best explained by the model. Therefore, the changes in the number of columns, column diameter, and column height are directly proportional to the changes in Ar value, Hp value, H-Dr value, Vr value, and the shear strength. While the confining pressures are directly proportional to the increment in the undrained shear strength value.

The study, therefore, concludes that the utilization of encapsulated bottom ash columns firmly influenced the engineering properties of the kaolin clay as an effective ground improvement. It is, therefore, recommended that single and group of encapsulated bottom ash columns with a 10-mm column diameter and 80-mm column height should be used by practitioners to improve the kaolin clay for construction application as the improvement to the ground can be reached up to 77.00%.

Acknowledgements The cooperation given by all parties involved in this research is greatly acknowledged.

Author contributions All authors contributed to the study conception and design. Material preparation, data collection, and analysis were performed by Muhammad Syamsul Imran Zaini, Muzamir Hasan, and Wan Nursyafiqah Binti Wan Jusoh. The first draft of the manuscript was written by Muhammad Syamsul Imran Zaini, and all authors commented on previous versions of the manuscript. All authors read and approved the final manuscript.

Funding The study leading to these results received funding from Universiti Malaysia Pahang (UMP) under Grant Agreement Numbers RDU202701, RDU223309, and PGRS2003185 and from Hokoku Engineering Co. Ltd. under Grant Agreement Number UIC201503.

Data availability All data generated or analyzed during this study are included in this published article.

Declarations

Ethical approval Not applicable

Consent to participate Not applicable

Consent for publication Not applicable

Conflict of interest The authors declare no competing interests.

References

- Ai X, Wang L, Xu D et al (2021) Stability of artificial soil aggregates for cut slope restoration: a case study from the subalpine zone of southwest China. *Soil Tillage Res.* <https://doi.org/10.1016/j.still.2021.104934>
- Ali B, Ouni M (2022) Kurda R (2022) Life cycle assessment (LCA) of precast concrete blocks utilizing ground granulated blast furnace slag. *Env Sci Pollut Res.* <https://doi.org/10.1007/s11356-022-21570-7>
- Bozyigit I, Javadi A, Altun S (2021) Strength properties of xanthan gum and guar gum treated kaolin at different water contents. *J Rock Mech Geotech Eng.* <https://doi.org/10.1016/j.jrmge.2021.06.007>
- Chemeda YC, Deneele D, Ouvrard G (2018) Short-term lime solution-kaolinite interfacial chemistry and its effect on long-term pozzolanic activity. *Appl Clay Sci.* <https://doi.org/10.1016/j.clay.2018.05.005>
- Choeycharoen P, Sornlar W, Wannagon A (2022) A sustainable bottom ash-based alkali-activated materials and geopolymers synthesized by using activator solutions from industrial wastes. *J Build Eng.* <https://doi.org/10.1016/j.job.2022.104659>
- Frikha W, Bouassida M, Canou J (2015) Parametric study of a clayey specimen reinforced by a granular column. *Int J Geomech.* [https://doi.org/10.1061/\(asce\)gm.1943-5622.0000419](https://doi.org/10.1061/(asce)gm.1943-5622.0000419)
- Gencil O, Balci B, Bayraktar O, Nodehi M, Sari A, Kaplan G, Hekimoglu G, Gholampour A, Benli A, Ozbakkaloglu T (2022) The effect of limestone and bottom ash sand with recycled fine aggregate in foam concrete. *J Build Eng.* <https://doi.org/10.1016/j.job.2022.104689>
- Hamada H, Alattar A, Tayeh B, Yahaya F, Adesina A (2022) Sustainable application of coal bottom ash as fine aggregates in concrete: a comprehensive review. *Case Stud Constr Mater.* <https://doi.org/10.1016/j.cscm.2022.e01109>
- Hamidi S, Marandi SM (2018) Clay concrete and effect of clay minerals types on stabilized soft clay soils by epoxy resin. *Appl Clay Sci.* <https://doi.org/10.1016/j.clay.2017.10.010>
- Hasan MB, Marto AB, Hyodo M, Makhtar AMB (2011) The strength of soft clay reinforced with singular and group bottom ash columns. *Electron J Geotech Eng* 16
- Hasan M, Zaini MSI, Yie LS et al (2021a) Effect of optimum utilization of silica fume and eggshell ash to the engineering properties of expansive soil. *J Mater Res Technol.* <https://doi.org/10.1016/j.jmrt.2021.07.023>
- Hasan M, Zaini MSI, Hong NAW et al (2021b) Sustainable ground improvement method using encapsulated polypropylene (PP) column reinforcement. In: IOP Conference Series: Earth and Environmental Science. <https://doi.org/10.1088/1755-1315/930/1/012016>
- Head KH (1982) Manual of soil laboratory testing, volume 2. Permeability, shear strength and compressibility tests. Man soil Lab testing, Vol 2 Permeability, Shear strength compressibility tests. [https://doi.org/10.1016/0016-7061\(95\)90001-2](https://doi.org/10.1016/0016-7061(95)90001-2)
- Hilal N, Hadzima-Nyarko M (2021) Improvement of eco-efficient self-compacting concrete manufacture by recycling high quantity of waste materials. *Environ Sci Pollut Res.* <https://doi.org/10.1007/s11356-021-14222-9>
- Hosseinpour I, Soriano C, Almeida MSS (2019) A comparative study for the performance of encased granular columns. *J Rock Mech Geotech Eng.* <https://doi.org/10.1016/j.jrmge.2018.12.002>
- Kererat C, Kroehong W, Thaipum S, Chindaprasirt P (2022) Bottom ash stabilized with cement and para rubber latex for road base applications. *Case Stud Constr Mater.* <https://doi.org/10.1016/j.cscm.2022.e01259>
- Khaw Le Ping K, Cheah C, Jia L, Siddique R, Tangchirapat W, Megat Johari MA (2022) Coal bottom ash as constituent binder and aggregate replacement in cementitious and geopolymer composites: a review. *J Build Eng.* <https://doi.org/10.1016/j.job.2022.104369>
- Kim B, Prezzi M, Salgado R (2005) Geotechnical properties of fly and bottom ash mixtures for use in highway embankments. *J Geotech Geoenvironmental Eng.* [https://doi.org/10.1061/\(asce\)1090-0241\(2005\)131:7\(914](https://doi.org/10.1061/(asce)1090-0241(2005)131:7(914)
- Mistry MK, Shukla SJ, Solanki CH (2021) Reuse of waste tyre products as a soil reinforcing material: a critical review. *Environ Sci Pollut Res.* <https://doi.org/10.1007/s11356-021-13522-4>
- Mohammed AMA, Mohd Yunus NZ, Hezmi MA et al (2021a) Carbonated ground granulated blast furnace slag stabilising brown kaolin. *Environ Sci Pollut Res.* <https://doi.org/10.1007/s11356-021-14718-4>
- Mohammed AMA, Mohd Yunus NZ, Hezmi MA et al (2021b) Ground improvement and its role in carbon dioxide reduction: a review. *Environ Sci Pollut Res.* <https://doi.org/10.1007/s11356-021-12392-0>
- Muhardi A, Marto A, Kassim KA et al (2010) Engineering characteristics of Tanjung Bin coal ash. *Electron J Geotech Eng* 15:1117–1129
- Muir-Wood D, Hu W, Nash DFT (2001) Group effects in stone column foundations: model tests. *Géotechnique.* <https://doi.org/10.1680/geot.51.7.649.51392>
- Nagy NM (2013) Numerical analysis of soft clay performance reinforced by geosynthetics encased stone columns. In: AIP Conference Proceedings. <https://doi.org/10.1063/1.4825926>
- Najjar SS, Sadek S, Maakaroun T (2010) Effect of sand columns on the undrained load response of soft clays. *J Geotech Geoenvironmental Eng.* [https://doi.org/10.1061/\(asce\)gt.1943-5606.0000328](https://doi.org/10.1061/(asce)gt.1943-5606.0000328)
- Orekanti ER, Dommaraju GV (2019) Load-settlement response of geotextile encased laterally reinforced granular piles in expansive

- soil under compression. *Int J Geosynth Gr Eng*. <https://doi.org/10.1007/s40891-019-0168-8>
- Phanikumar BR, Ramanjaneya Raju E (2020) Compaction and strength characteristics of an expansive clay stabilised with lime sludge and cement. *Soils Found*. <https://doi.org/10.1016/j.sandf.2020.01.007>
- Prasad SSG, Satyanarayana PVV (2021) Stabilization of soft soils using single and group of sand columns. In: *Lecture Notes in Civil Engineering*. https://doi.org/10.1007/978-981-33-4590-4_35
- Rezaei-Hosseiniabadi MJ, Bayat M, Nadi B, Rahimi A (2022a) Utilisation of steel slag as a granular column to enhance the lateral load capacity of soil. *Geomech Geoenviron*. <https://doi.org/10.1080/17486025.2021.1940315>
- Rezaei-Hosseiniabadi MJ, Bayat M, Nadi B, Rahimi A (2022b) Sustainable utilisation of steel slag as granular column for ground improvement in geotechnical projects. *Case Stud Constr Mater*. <https://doi.org/10.1016/j.cscm.2022.e01333>
- Russo F, Veropalumbo R, Oretto C, Cassese D, Papa B, Malvezzi S (2022) Reusing bottom ash as a filler from a waste-to-energy plant for making asphalt mastics. *Case Stud Constr Mater*. <https://doi.org/10.1016/j.cscm.2022.e01406>
- Singh M, Siddique R (2015) Properties of concrete containing high volumes of coal bottom ash as fine aggregate. *J Clean Prod*. <https://doi.org/10.1016/j.jclepro.2014.12.026>
- Singh A, Zhou Y, Gupta V, Sharma R (2022) Sustainable use of different size fractions of municipal solid waste incinerator bottom ash and recycled fine aggregates in cement mortar. *Case Stud Constr Mater*. <https://doi.org/10.1016/j.cscm.2022.e01434>
- Tambara Júnior LUD, Taborda-Barraza M, Cheriaf M et al (2022) Effect of bottom ash waste on the rheology and durability of alkali activation pastes. *Case Stud Constr Mater*. <https://doi.org/10.1016/j.cscm.2021.e00790>
- Tandel YK., Solanki CH, Desai AK (2012) Numerical modelling of encapsulated stone column-reinforced ground. *Int J Civil Struct Environ Infrastruct Eng* 2(1), 82-96.
- Ul Haq E, Kunjalukkal Padmanabhan S, Licciulli A (2014) Synthesis and characteristics of fly ash and bottom ash based geopolymers—a comparative study. *Ceram Int*. <https://doi.org/10.1016/j.ceramint.2013.10.012>
- Vakalova T, Pogrebenkov V, Vereshagin V et al (2018) Optimising rational chemical analysis for quantitative determination of the composition of clay in soils. *Appl Clay Sci*. <https://doi.org/10.1016/j.clay.2018.07.014>
- Verma P, Sahu AK (2019) Effect of grouted granular column on the load carrying capacity of the expansive soil. *Int J Recent Technol Eng*. <https://doi.org/10.35940/ijrte.C4924.098319>
- Wang L, Zhou A, Xu Y, Xia X (2022) Consolidation of partially saturated ground improved by impervious column inclusion: governing equations and semi-analytical solutions. *J Rock Mech Geotech Eng*. <https://doi.org/10.1016/j.jrmge.2021.09.017>
- Xue S, Huang N, Fan J et al (2021) Evaluation of aggregate formation, stability and pore characteristics of bauxite residue following polymer materials addition. *Sci Total Environ*. <https://doi.org/10.1016/j.scitotenv.2020.142750>
- Zaini MSI, Hasan M, Yie LS et al (2022a) The effect of utilizing silica fume and eggshell ash on the geotechnical properties of soft kaolin clay. *J Teknol*. <https://doi.org/10.11113/jurnalteknologi.v84.17115>
- Zaini MSI, Hasan M, Zolkepli MF (2022b) Urban landfills investigation for leachate assessment using electrical resistivity imaging in Johor, Malaysia. *Environ Challenges*. <https://doi.org/10.1016/j.envc.2021.100415>

Publisher's note Springer Nature remains neutral with regard to jurisdictional claims in published maps and institutional affiliations.

Springer Nature or its licensor (e.g. a society or other partner) holds exclusive rights to this article under a publishing agreement with the author(s) or other rightsholder(s); author self-archiving of the accepted manuscript version of this article is solely governed by the terms of such publishing agreement and applicable law.